# CHAPTER II

## THE TELESCOPE DESIGN

### 1. General Description

Figures 2 and 3 show two outline drawings of the telescope. It is an altitude-azimuth instrument; one in which the whole structure rotates in azimuth on rail tracks about a central pintle bearing. The reflector can be rotated about a horizontal elevation axis between two bearings carried at the top of the support towers. The telescope is driven in azimuth by electric motors geared to the wheels on the azimuth track and in elevation by motors geared to pinions which drive a bull gear on the elevation wheel. Control by a high-speed computer system allows the telescope to slew, scan and track under servo-mechanism control at a wide range of rates.

The optics of the instrument can be either Cassegrain or prime focus. When used as a Cassegrain, the radio waves reflected from the main 65-meter parabolic reflector are reflected a second time at a much smaller diameter (12 feet or 3.7 meters) hyperboloid mirror (subreflector) which is near the focal point of the main mirror. The radio energy is then focussed to the feed horn in the main equipment cabin in the center of the parabolic reflector. For use as a prime focus instrument, the subreflector is removed and the energy is collected by a feed horn in the equipment room at the vertex of the feed support legs.

Thus duality of methods of using the telescope is of great value since for very short wavelength work the Cassegrain mode is most desirable while, if research is to be done at wavelengths longer than a few centimeters, the prime focus mode is generally more practical.

### 2. Rotation in Azimuth (SDL Report No. H-10, Sections 4 and 5)*

The main components which provide for the azimuth rotation are the telescope foundation, on which the azimuth rails are mounted, the

---

* References of this kind indicate the source of the original design material; to locate it see the final section entitled Appendices.

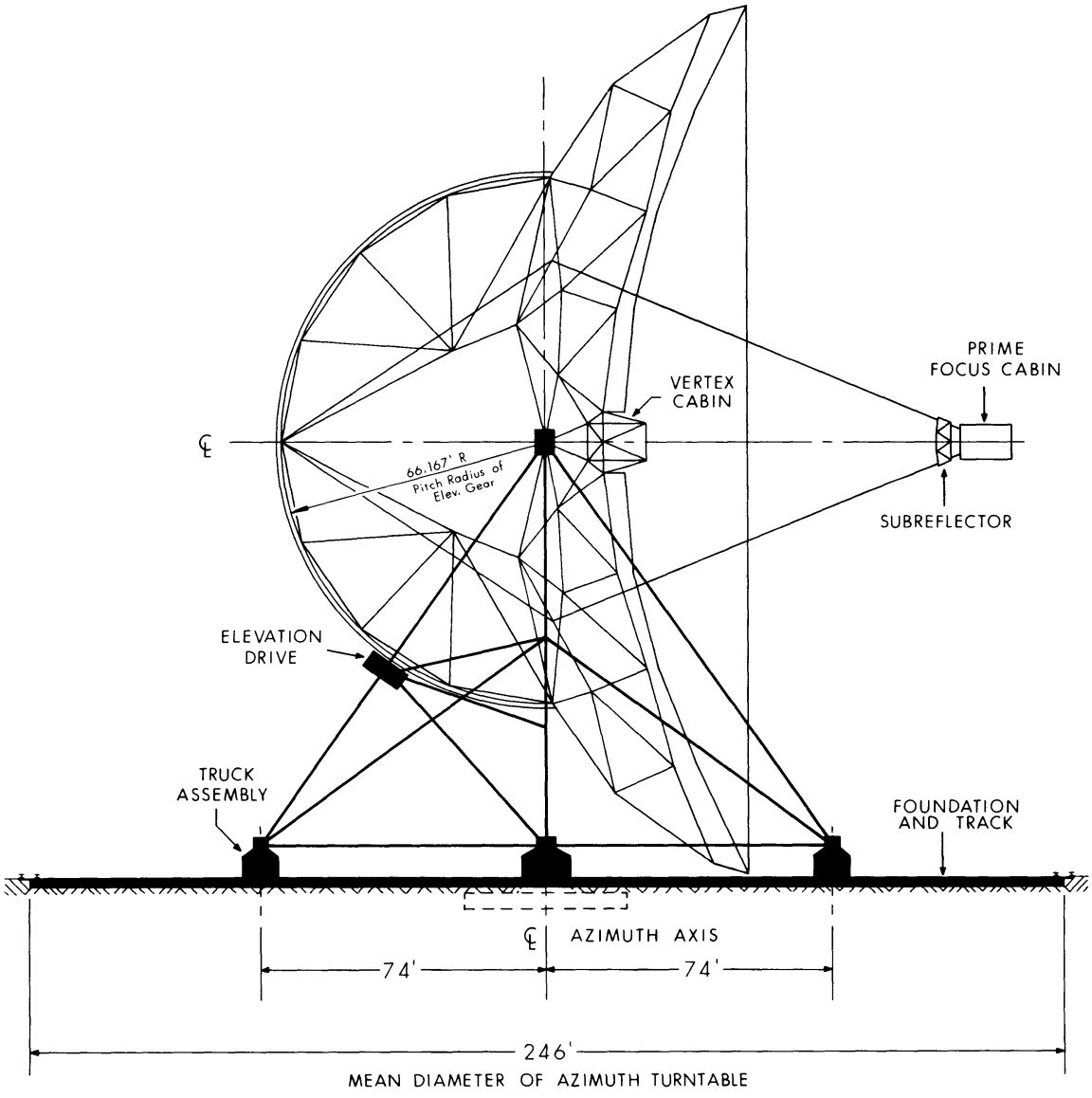


Figure 2. Outline drawing of the telescope--horizon position.

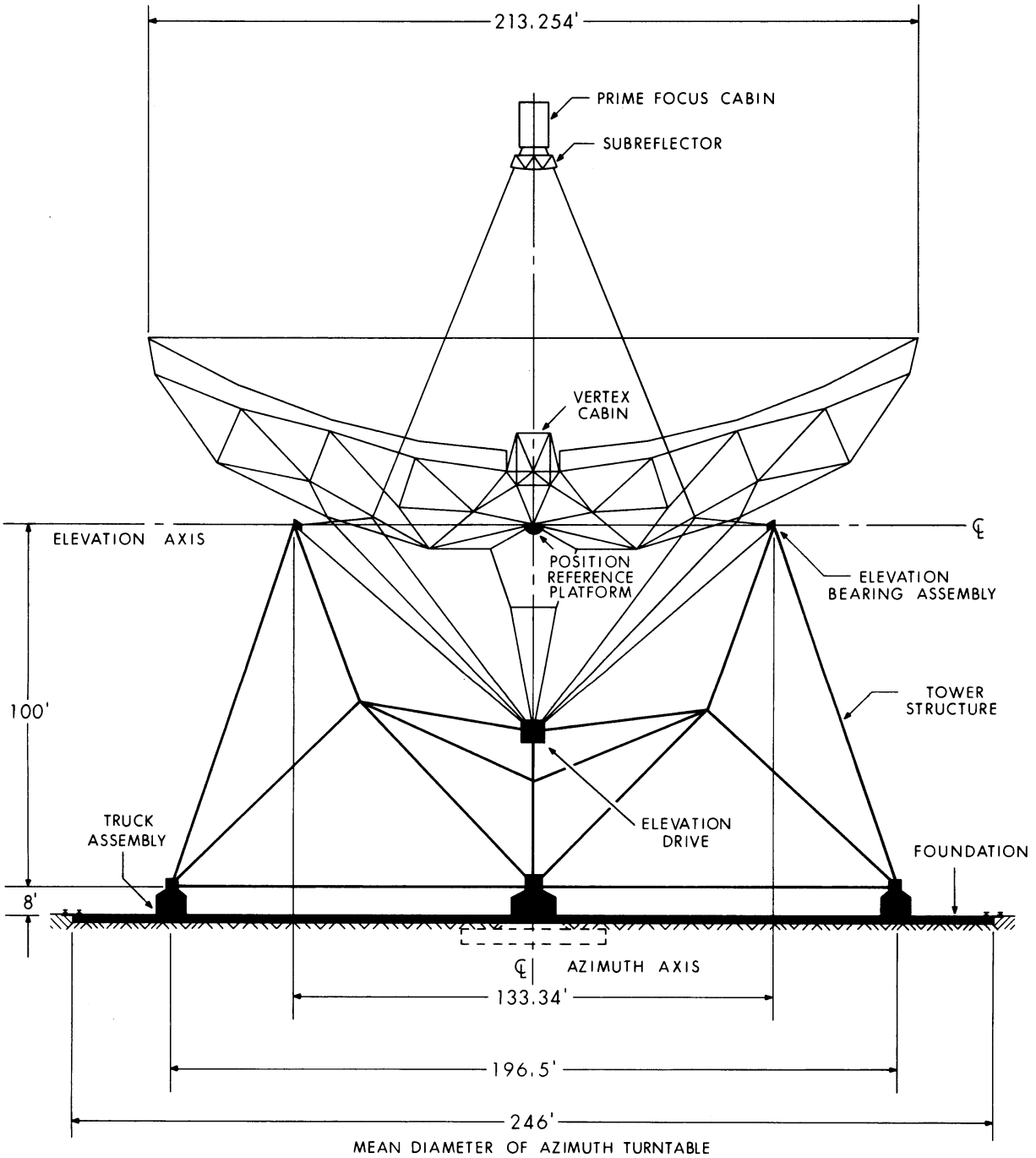


Figure 3. Outline drawing of the telescope--zenith position.

trucks with their drive motors, gear trains and brakes and the central pintle bearing. Precise knowledge of the azimuth pointing is derived from the reference platform, but pointing is also measured with lower precision by an encoder mounted at the pintle bearing.

(a) The telescope foundation and rails. The foundation is a ring of concrete with steel reinforcement 9 feet wide and 2 feet deep with a mean radius of 123 feet. This supports the rail track, which is made of two concentric circles of 175-CR crane rail giving a 5-foot width for the rail track. Figure 4 shows details of how the rail (which is crowned) is mounted on the foundation. The top surface of the rails will be set and maintained level to ± 0.125 inches (3.2 mm) by shims. This accuracy is not difficult to achieve and is desirable to give smooth rotation for the azimuth drive. There are six positions around the rail where the trucks can be tied to the foundation (for stowing the telescope in high winds).

The foundation and rail has to be adequately strong to carry the telescope loads, and it must also resist deflections (be stiff enough) so as not to contribute much to the flexibility of the structure in any dynamic modes. In fact, from both these points of view, the foundation and rail is somewhat over-designed, since it has been derived from the work done for the earlier 300-foot telescope design*. The design will be reviewed when subsurface conditions at the selected site are known.

(b) The azimuth trucks. Four trucks, each of which has eight wheels, carry the whole moving weight and other vertical telescope loads to the tracks. These trucks also carry the azimuth drive motors, gear trains and brakes; the drive forces are provided by the friction between the driven wheels and the rails. Each truck may experience a maximum vertical load of about 500 tons; again, as in the case of the foundation, the actual design is conservative and capable of carrying greater loads. Figure 5 shows the side view of a truck; further details are on Drawing No. 111-D-008, Sheets 1-3.

Several important requirements have to be met by the trucks, and these have all been allowed for in the design. The load on any one truck must be fairly evenly divided between the eight wheels, even when the rail top surface is not exactly level and when it deflects under load. Each truck must provide for a braking force onto the rail, so that the telescope can be held still with the wheel loads reduced. The four driven wheels must be so arranged that when the telescope is being driven the drive force at a wheel must be tangential to the wheel and lie in the plane of the wheel. The frictional forces between the wheels and the rail in both the static and the rolling cases must not be too great; nor must the difference between static and rolling friction be too large.

---

* A 300-foot High-Precision Radio Telescope, National Radio Astronomy Observatory, May 1969.

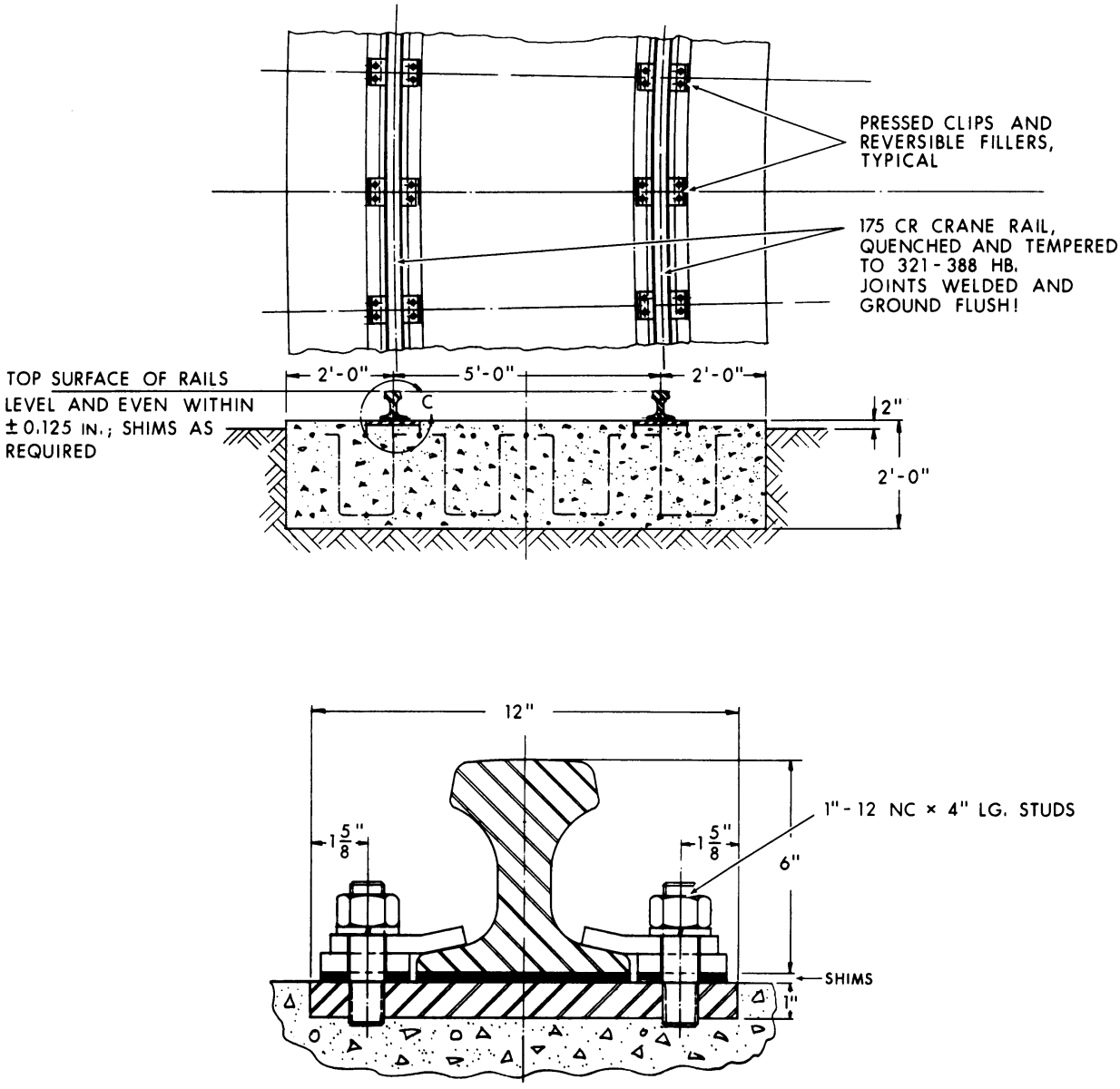


Figure 4. The azimuth track and rails.

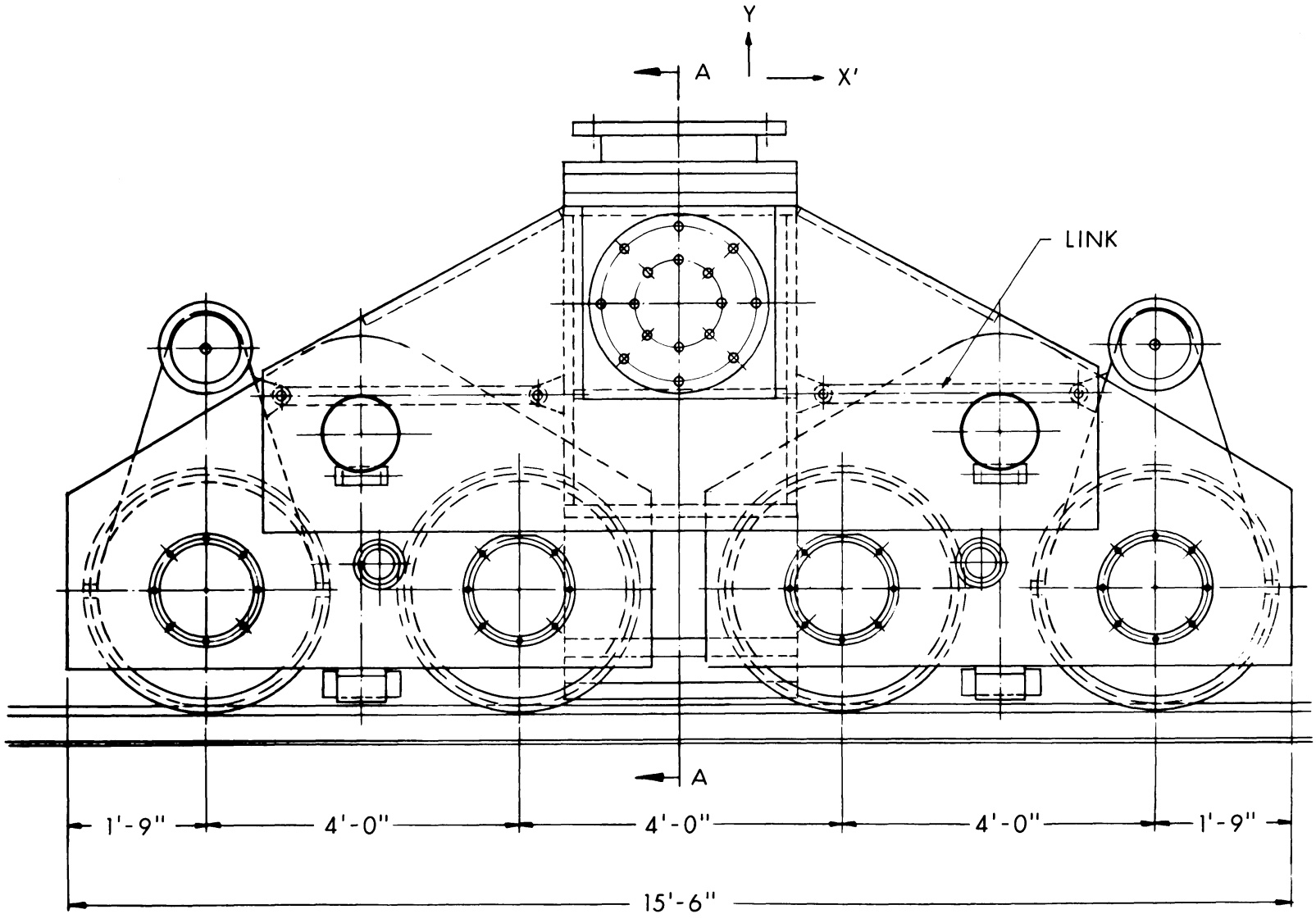


Figure 5. The side view of an azimuth truck.

The other important components in the trucks are the DC servo motors and gear trains. These are described further under the drive and control system.

(c) The pintle bearing and cable-twist. The whole structure rotates about the pintle bearing as its center, and this bearing has to withstand any lateral forces which are given to the telescope by winds. Although, in principle, the pintle bearing need carry no other loads, the present design does allow the bearing to carry some part of the vertical loads due to the weight of the tower. Also, since the azimuth track does not lie exactly in a plane, the bearing must accept loads due to small tilts of the structure as well as the lateral wind-generated loads.

Accordingly, a preloaded, self-aligning bearing has been designed which can take both up and down vertical loads, radial loads and any alignment moments generated as the structure rotates. The preload eliminates play; to meet the load requirements a combination of a self-aligning spherical roller thrust bearing preloaded by a self-aligning cylindrical thrust bearing is used. The alignment surface curvatures of the two bearings coincide. The detailed design of the bearing is given on Drawing 111-D-006.

The azimuth cabling of the telescope passes through a 24-inch diameter hole in the center of this bearing; this in turn requires that the coarse azimuth encoder be gear driven and not axially mounted, but adequate accuracy can be achieved by this method of encoder drive.

The cables from the moving parts of the telescope pass to the fixed ground through the cable-twist. In the present design, the bundle of cables 60 feet long is suspended through the central tower member, through the pintle bearing and down to a point 30 feet below ground. The $\pm$ 270° rotation of the telescope twists this bundle, rather than using a wind-up drum. This feature and the straightforward pintle-bearing foundation are shown in Drawing 111-D-004.

3. The Tower Structure and Elevation Bearings (SDL Report H-10, Chapters 3 and 6)

(a) The tower structure. The main function of the towers is to provide the support structure between the elevation bearings (which carry the reflector) and the azimuth trucks and pintle bearing. However, there are various further demands placed on the tower, and the design has been made to satisfy all these requirements. For example, the tower structure must:

(i) Have reasonably small deflections due to wind forces.
(ii) Meet the survival loads imposed on it.
(iii) Give a satisfactory dynamic behavior for the telescope structure.

(iv) Not impose any stresses on the reflector under normal operating conditions which could distort the reflector beyond the limits set by the shortest usable wavelength of the telescope

(v) Block as little as possible the light beams in their paths from the ground-based autocollimators to the mirrors on the reference platform.

The tower structure which meets these requirements is an improvement on the structure designed earlier for the 300-foot antenna. The base configuration has been simplified; the lower weight permits the use of only four trucks and welded tubular members have been chosen for the structure. The details of the tower are shown in Drawings 111-D-002, Sheets 1-3. The total weight of structural steel in the tower is 366 tons. The dynamic properties of the tower are discussed later in this report.

(b) The elevation bearings. For the optimum performance of the homologous reflector, it is necessary that applied or reacted forces and moments imposed at the elevation bearings be kept at the lowest possible levels in order to minimize secondary, unpredictable surface deformations.

For these reasons, the design concept for the elevation bearing, as shown in Figure 6, is proposed. The scheme is somewhat unusual because of the application of a pair of axially preloaded spherical roller thrust bearings which act as primary radial bearings. However, because of this particular arrangement, which permits a common center of the spherical radius for each set of opposing bearings, nearly equal load sharing as well as freedom of spherical rotation of each elevation bearing assembly is essentially assured. Thus, only a small frictional alignment moment is transferred into the reflector structure by either load flexures of the tower structure in the elevation axis direction or by bearing misalignments.

Because of axial preload requirement, the U-shaped bearing housing becomes rather heavy in proportion to other structural components. However, stiffness is of primary interest in this case and takes preference over weight or size considerations.

Nevertheless, it may well be possible to reduce both size and weight of the bearing assemblies during the final design stage, subject to a trade-off study of stiffness requirements versus system dynamics requirements, as the design shown in Figure 6 was originally prepared for the 300-foot diameter telescope and, therefore, is somewhat oversized.

## 4. The Reflector Structure, the Spherical Joints and the Panels

(a) The reflector structure (W-Y. Wong Reports 34 and 34A). This is the structure which is supported on the elevation bearings; it

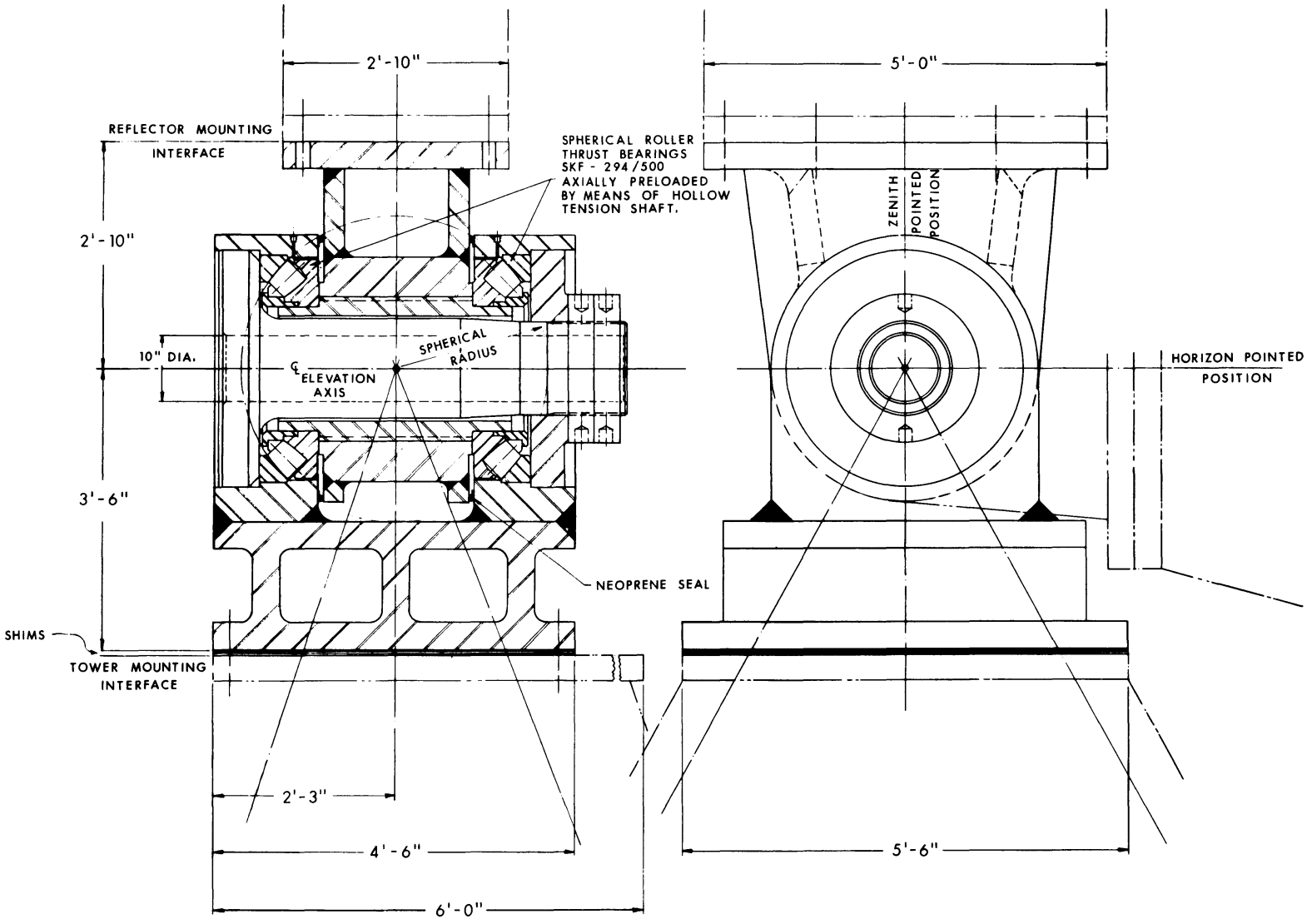


Figure 6. The elevation bearings.

includes the elevation drive wheel structure but does not include the feed support legs. Its function is to give the main support for the reflector surface. This main support is provided at 60 homologous points. These 60 points (which are radially symmetrically placed, see Figure 7) in turn are bridged by the panel structures and finally the surface plates are supported on the panels. This nomenclature should be noted, since the word "panel" is used by some engineers to mean the reflecting surface itself. The panels are described later in this section; here it is only necessary to say that they have linear dimensions of the order of 30 feet and thus are important structures in their own right.

The reflector structure is homologous; as its elevation angle changes the 60 main surface joints always remain very closely on a parabolic surface. The focal length of this surface changes regularly with elevation angle and so also does the departure of the direction of its axis of symmetry from the direction defined by the elevation axis position encoder.

The way in which von Hoerner's method achieves homologous performance has been published (von Hoerner 1967(b) and 1969) and will not be repeated. The application of it to the present design has been straightforward; the following conditions have been included in the design and have been satisfactorily met.

(i) The 60 homologous points must remain at their required position to an RMS accuracy of 0.004 inches (0.10 mm) as the telescope tilts from zenith to horizon.

(ii) All expected dead loads must be applied to the structure in its design. These loads include the surface panel and plate loads and the loads imposed by the feed legs, the prime focus and the vertex equipment rooms. The loads from the elevation drive have been arranged to be small.

(iii) The design must allow for the selection of member sizes, which in as many cases as possible are standard sized tubes or pipes. It must show separately those members which have to be specially fabricated. The effects on homology of this selection must be checked.

(iv) The structural design must include the weights and stiffness of the spherical joints (see Section 4(b)) for their effects on strength and homology.

(v) The structural design must be one which is practical for fabrication and erection.

(vi) The design must produce a structure which meets the survival conditions imposed by high winds and possible snow or ice loading.

(vii) The structure must have adequate stiffness so that its overall and detailed dynamic behavior is satisfactory.

The design and computational work which has been needed to achieve these results is very extensive. The results are summarized in W-Y.

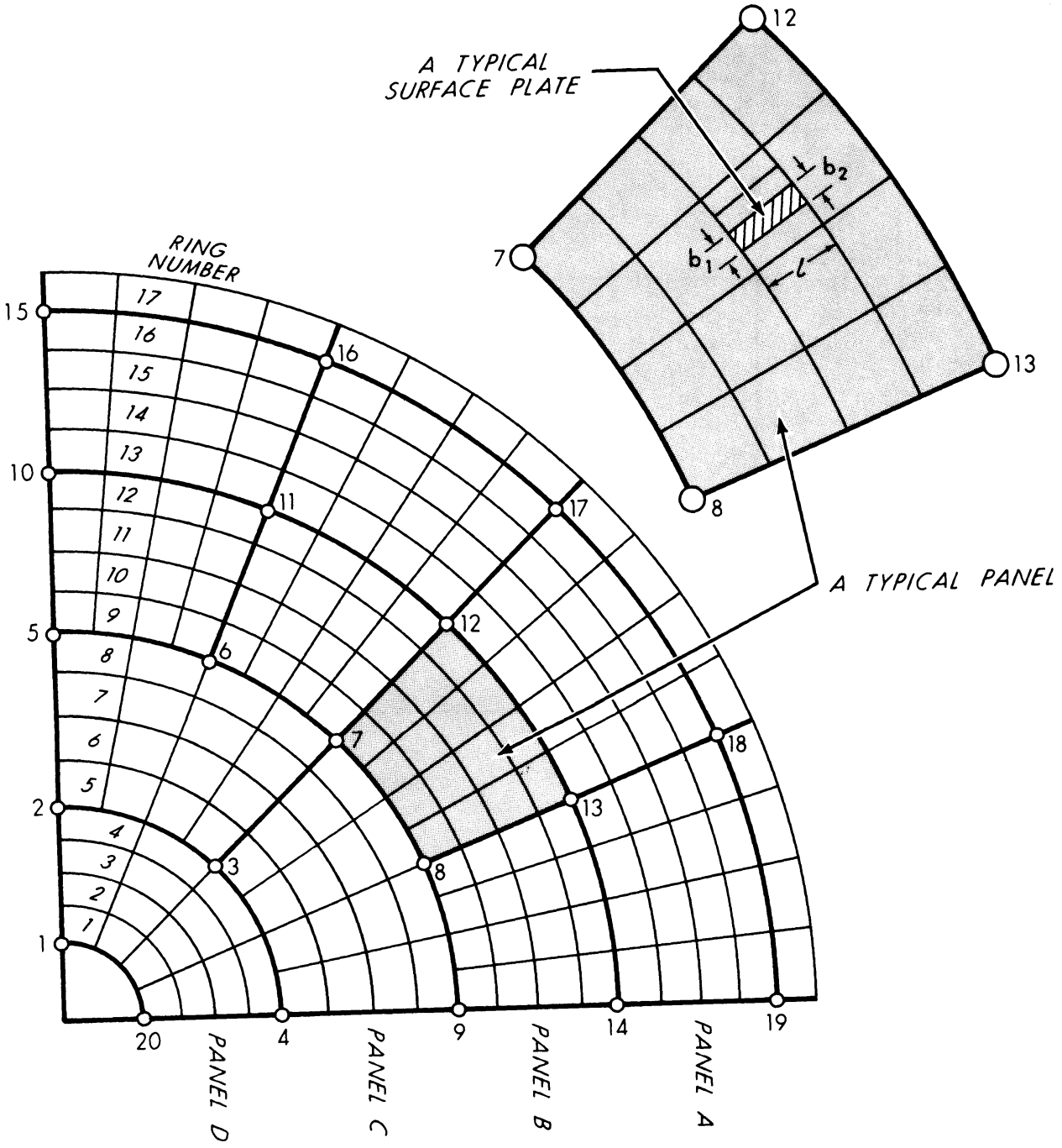


Figure 7. The homologous joints which support the panel structures.

Wong's Reports 34 and 34A. The accuracies to be expected from the reflector design are considered in more detail in Chapter III.

The choice of tubes and pipes is economical for several reasons, but raises the possibility of individual member vibrations induced by even quite moderate winds. This type of vibration is well-known. For the present structure, it has been considered (S. von Hoerner Reports Nos. 24 and 35). Wind-induced vibrations are not critical if the wind velocity which makes the member resonant is above the greatest velocity expected or if the air flow is turbulent. If these conditions are not met, members will vibrate at their natural frequencies so that under this condition the alternating stress in the member must be low enough to avoid fatigue failure even with any number of oscillations. The structure has been checked to ensure that no members are unsafe due to wind-induced vibrations.

The reflector structure is specified in detail in W-Y. Wong's Reports 34 and 34A. These give joint coordinates, member sizes and say which members are standard, which have to be specially ordered and which are to be individually fabricated. The reflector design is shown in Drawings D-111-001, Sheets 1-6.

The designs for both the tower and reflector structure have been made with the intent of using a steel of high yield strength. One such material is Cor-Ten* manufactured by U.S. Steel. This steel also has good resistance against corrosion. The latter property will be important in that no serious loss of cross-section area (which might be important in some thin-walled sections) can occur due to corrosion of the interior of the members. All exterior surfaces will be protected by paint; this is needed for temperature control. Furthermore, corrosion-resistant steels require painting less often than more normal varieties and thus give a maintenance advantage. Although Cor-Ten is discussed here, the design requirements can be met also by steel of approximately equivalent properties available from other steel producers.

(b) The spherical joints (SDL Report H-10, Chapter 2). The use of tubular members in radio telescopes is well established; both the Parkes 210-foot and the Effelsberg 100-meter instruments use many such members. However, in the present design their use, and the following other factors, require the adoption of a somewhat unusual joint design. For example, in the reflector structure most members connecting at a particular joint are not oriented in common planes, as is the case with most standard space frames, but project from all directions since the joint locations are dictated by the requirements for a homologous deformation solution and not by geometrical considerations alone. Furthermore, in some instances as many as 15 members intersect at one point, which makes it impractical to employ direct or gusset plate joint connection of the tubular members.

---

* Cor-Ten is a trade-mark of U. S. Steel.

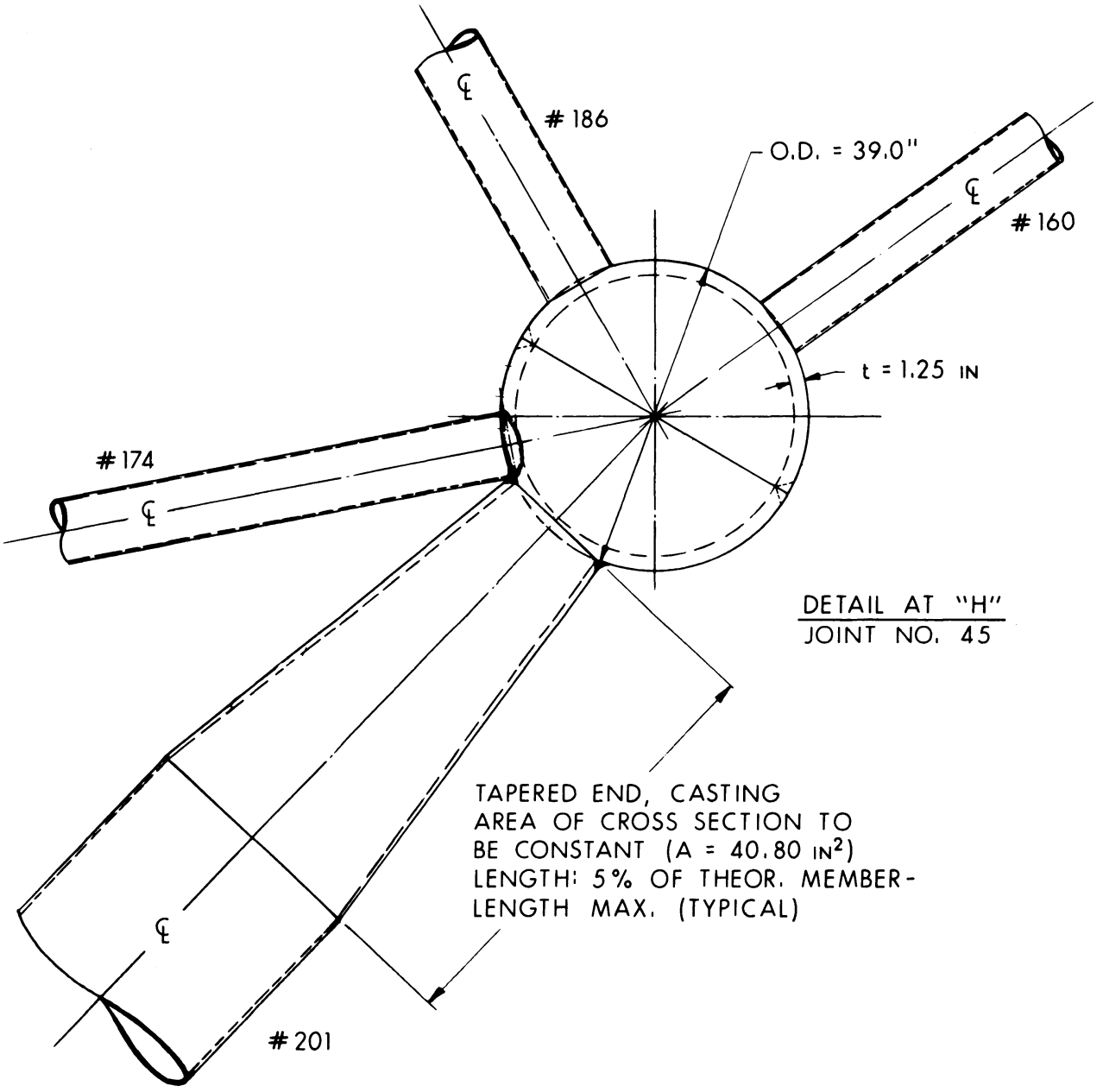


Figure 8. An example of a spherical joint (No. 45) in the reflector.

Also, to ensure that homology was maintained in the reflector design it was necessary that the additional total joint weight be limited to about 3 percent of the total reflector weight and that the average axial stiffness variation of each joint member connection be no more than ± 5 percent of the theoretical stiffnesses of an idealized structure consisting of full length members and pin joints.

Another requirement was that the axial offset of each member from the theoretical point of intersection be kept as small as possible so as to minimize the effects of secondary moments acting on the joints which could also possibly alter the homologous reflector deformations. Finally, connections and alignments of members must be easy and the joint design should preferably be universal in order to be economical.

The concept of joints which are hollow spherical shells, of correctly chosen diameters and wall thickness, has been adopted and meets the foregoing requirements. Such a concept is not new; one example is to be found in the truss structure for the Japanese built roof of Expo 70's "Symbol Zone".

Two computer programs have been used to determine the geometry, strength and stiffness of the joints. One determined the angles between members and derived the minimum possible sphere diameters. The second program determined the joint stresses, wall thicknesses, stiffnesses and weights.

The joints replace the end parts of the members of the reflector structure, but the knowledge of their weights and stiffnesses, as compared to the same quantities for the pieces of steel they replace, allow for the homology solution to be rechecked. This has been done and the deviations produced are acceptable. The following table summarizes the results of the reflector joint design.

| | | |
|---|---|---|
| Total number of spherical shells required | : | 145 |
| Estimated total shell weight | : | 33 tons |
| Net weight increase, due to replacing member ends with joints | : | 20 tons |
| Maximum stress in joints | : | below 19,000 $lbs/in^2$ |

Figure 8 shows an example of one of the joints for the reflector structure. The tower structure is less complex than the reflector and conventional welded joints are used.

The methods of fabricating the joints have been studied and seem straightforward. The shells will be cast in two halves using Austenetic Manganese Steel (ASTM-A-128-64) which has a yield strength of more than 50,000 $lbs/in^2$ and which is weldable to Cor-Ten. The two half spheres are welded together and member ends (which will be tapered castings if neces-

sary) are welded to the spheres. Complete joints will be stress-relieved in the fabrication shop.

(c) The panels (Collins Yang and S. von Hoerner, Reports Nos. 40 and 41). The panels bridge the 60 homologous reflector structure points (Figure 7) and in turn each panel carries between 56 and 80 reflector surface plates. The radially symmetric arrangement of the 60 homologous points means that four panel designs only are required--an outer ring of 16 (Panel A, the next ring of 16 (Panel B), the next ring of 8 (Panel C) and the inner ring of 4 (Panel D).

The requirements placed on the panels are quite strict, as the following list shows, and their design was a considerable task in structural design and analysis. The panels must:

(i) Carry the homologous behavior of their 60 support points through to the points of attachment of the surface plates to the panels. This must be realized under the applied loads of their own dead load, the surface plate dead load and the loads imposed on the panels by the reflector structure as it in turn deflects.

(ii) Maintain the accuracy of the surface plate support positions under operating wind conditions.

(iii) Be adequately strong to withstand survival loads due to wind, snow or ice.

Most of the design problems arose in meeting the first of these conditions. Two principles were followed: (1) The dead loads should move the surface plate points by equal amounts in a direction parallel to the reflector axis and (2) the forces exerted on the corners of the panels by the rest of the reflector structure should not move the surface points at all in this same direction. These conditions were met by using the concepts (von Hoerner 1967(a) of "equal softness" for (1) and "pressure-stable cells" for (2). The analysis used in the design was "trial and success" rather than an attempt to use a complete homology program, since the required accuracy could be met by this method. A standard structural analysis computer program was used throughout the analysis, but the final designs were reanalyzed by using frame and truss models, which gave very similar results. Since a truss model assumes a pin-jointed structure and a frame model allows for joint stiffness, their agreement shows that joint stiffness is unimportant.

Figure 9 is an example of one of the results of this process; it shows the geometry of the members which go into each of the 16 "B" panels. Report No. 40 gives the detailed results (in the form of joint coordinates and member sizes) for each of the four types of panel.

The panels will be fabricated from Cor-Ten pipe. No complications are expected for the internal joints; the connections between the panels and the 60 reflector structure points have been given special consideration and a suitable welded connection has been proposed.

The performance of the panels under dead loads, operating wind forces and thermal effects has been evaluated and the results are

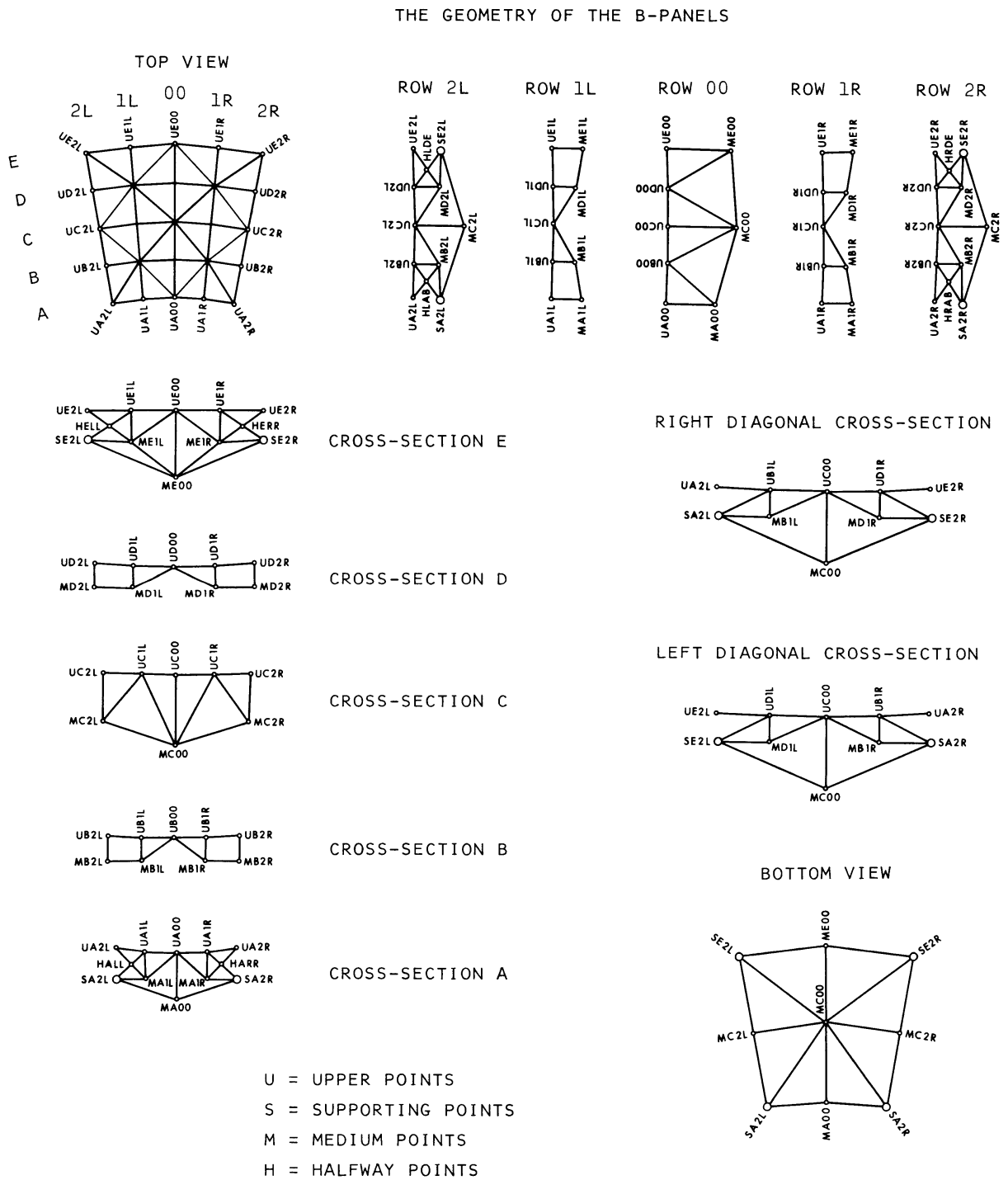


Figure 9. The geometry of the B-panels.

included in Chapter III. It is sufficient to note here that the dead-load panel deflections add an RMS inaccuracy of 0.002 inches (0.051 mm) to the overall surface accuracy. Similarly, the adequacy of the design to meet the survival conditions has also been satisfactorily determined.

5. The Surface Plates, Their Fabrication and Setting

(a) The requirements the plates must meet. The reflecting surface of the telescope is formed by the surface plates, each of which is mounted by adjustable screw jacks to the panel structures. In a highly precise telescope the surface plates must meet a set of demanding requirements.

(i) The individual plates must have a high-reflection coefficient and a very small transmission coefficient for millimeter-wave radio waves.

(ii) The shape of each plate must conform closely to the shape of that part of the parabolic surface it represents. The shape should not deform seriously under operating wind and temperature conditions. The shape may deform under the survival snow, ice, and wind loads, but the plates, after such loading, must return accurately to their original shape.

(iii) The surface plates must be capable of being manufactured at reasonable cost. They must be capable of being transported to the telescope and mounted on their panel support points without undue risk of damage or loss of surface accuracy, nor must these operations be unduly expensive.

(iv) A means must be found whereby the plates can be measured and adjusted after they have been mounted on the telescope to conform to the parabolic reflector surface with the required accuracy. (This is a requirement for an accurate measuring technique rather than for a property of the plates themselves. It does, however, affect some characteristics of the plates.)

(b) Meeting the requirements. The first requirement is easily met if the reflector surface is a good, highly conducting sheet of metal without holes or large gaps. The use of very fine mesh or perforated sheet would be possible, but for millimeter wavelengths the holes have to be so small that no appreciable reduction of wind forces results. Equally, very mild ice or snow conditions easily block such fine holes. Therefore, solid aluminum is selected for the plates. This requires that the corner mounting arrangements must allow for the differential expansion of the surface plate and its steel support structure. This the present design does satisfactorily. To keep radio leakage low, the gaps between the plates, when mounted on the telescope, are kept to about 1.5 mm (0.06 inches). This is adequate to avoid appreciable loss of antenna gain or any noticeable increase of antenna temperature due to ground

radiation reaching the receiving horn through the surface of the reflector.

Meeting the next three conditions has required a considerable amount of work; the performance of the instrument and its cost depend heavily on the success achieved. Therefore, more than one solution has been sought, and in what follows we will describe the two most attractive of these solutions.

To indicate the importance of the problem, we set out in Table 4 below reasonable estimates of the likely contributions to the surface error budget which may be allowed to arise from the surface plates.

Table 4. Estimated Surface Error Budget for the Reflector Surface Plates

| Source of Error | Estimated RMS Error |
|---|---|
| Fabrication and test of surface plates at the manufacturer | ± 0.003 inch<br>± 0.076 mm |
| Setting accuracy of the plates on the telescope | ± 0.005 inch<br>± 0.127 mm |
| Root sum square value of all other contributions (subreflector, gravity, wind and temperature effects on the plates and structure) | ± 0.006 inch |

In Chapter III, we summarize the surface error budget which we expect the telescope to meet, and Table 4 is only presented here to show what small parts of the total are likely to be permissible for the surface plate fabrication and setting. The root sum square of the figures in the last column is 0.212 mm, approximately the design figure given in Table 1, so that the surface plates must be fabricated and set to about the accuracies given in Table 4.

(c) The NRAO surface plate (S. von Hoerner Report No. 38). A design for a surface plate has been made at NRAO and typical plates have been fabricated and tested. The results show that such plates meet the requirements already stated. The work has been extensive and the final results are given in the above-referenced report.

The surface of the telescope will consist of 17 concentric rings of surface plates (see Figure 7); the total number of plates is 2912. Most of the plates have a length of about 74 inches; the four inner rings have plate lengths of about 63 inches; the widths of the plates vary from ring to ring. As the following Table 5 shows, between 32 and 256 plates

fall into each of the 17 groups of plates. The total surface area of the plates is 38,258 sq. feet (3554 sq. meters).

Table 5. The 17 Groups of Surface Plates

| Ring Number | No. of Plates in Ring | Length of Plate | Width of Plates in Inches Lower Edge | Upper Edge |
|---|---|---|---|---|
| 1 | 32 | | 25.5 | 37.9 |
| 2 | 64 | 63.08 inches | 18.9 | 31.2 |
| 3 | 64 | | 25.1 | 31.2 |
| 4 | 64 | | 31.2 | 37.4 |
| 5 | 128 | | 18.7 | 22.3 |
| 6 | 128 | | 22.3 | 25.8 |
| 7 | 128 | | 25.8 | 29.4 |
| 8 | 128 | | 29.4 | 32.9 |
| 9 | 128 | | 32.9 | 36.3 |
| 10 | 256 | 74.39 | 18.2 | 19.9 |
| 11 | 256 | | 19.9 | 21.6 |
| 12 | 256 | | 21.6 | 23.3 |
| 13 | 256 | | 23.3 | 24.9 |
| 14 | 256 | | 24.9 | 26.6 |
| 15 | 256 | | 26.6 | 28.2 |
| 16 | 256 | | 28.2 | 29.8 |
| 17 | 256 | | 29.8 | 31.4 |

The design of the NRAO surface plate is shown in Figure 10, and one of the test plates is shown in Plates 2 and 3. The engineering drawing of a test plate (56D00086) is in the Appendices. The plate is made of an aluminum skin, 0.125 inches thick, supported by a series of upper ribs riveted to the skin and then by a system of lower ribs below the skin. All ribs are aluminum. The upper ribs and skin are connected to the lower ribs by a total of 36 adjustment screws; by turning these screws the surface plate is adjusted to conform to the required shape. The skin before adjustment is a routinely manufactured flat sheet. The design has been evolved by various tests made on specimen surface plates with various detailed differences in design. The best design was adjusted and tested as follows:

(i) The adjustment screws were roughly set by bending the surface plate over a rod placed first along its long center line, then along its short center line.

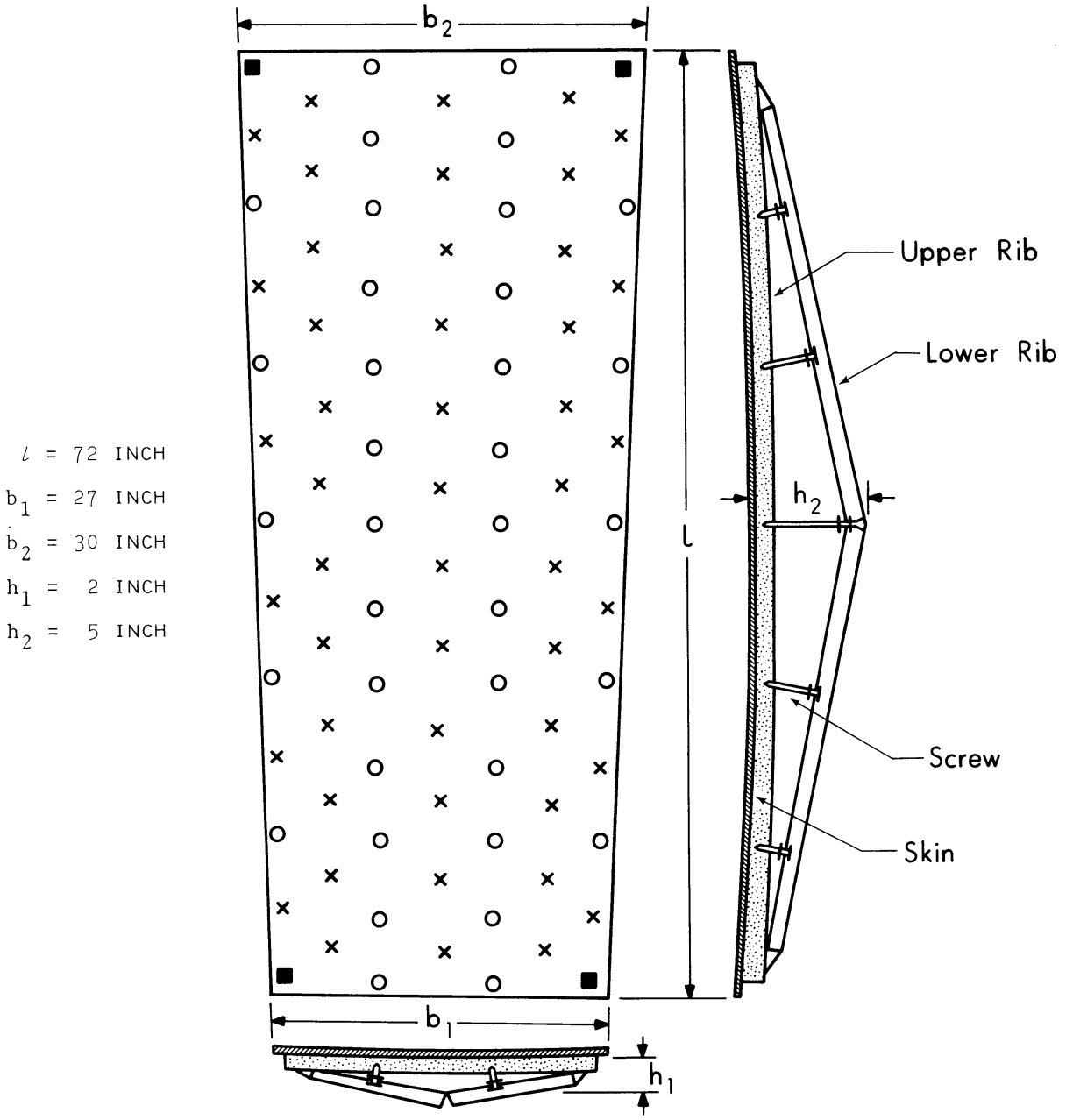


Figure 10. The NRAO surface plate.

Plate 3. Photograph of the NRAO surface plate.

Plate 2. Photograph of the NRAO surface plate.

(ii) Individual adjustments were made to the 36 screws; the surface was supported at its four corners (arranged to lie in a horizontal plane) and the surface contour was measured using a precise level and vertical scale. The measurement accuracy of this system (RMS value of repeatability) was ± 0.0006 inches (± 0.015 mm). A total of 88 points were measured on the surface (see Figure 10). After adjustment a typical value for the RMS value of the departures from true parabolic shape was 0.0024 inch (0.061 mm). The adjustment screws were locked by an epoxy cement when the adjustment process ended.

(iii) Hysteresis effects due to heavy loads were investigated by having a man walk on the plate. The plate was mounted skin up on its four corners, walked on for a few minutes and measured on its measurement jig. The plate was turned over and the process repeated. The whole cycle was repeated five times. From the skin-up and skin-down measurements, the RMS departure from its original shape was found to be 0.00067 inch (0.017 mm). This showed that for such loads (which exceed 200 pounds per square foot) the plates deform elastically and return very accurately to their original shape when the load is removed.

(iv) Gravitational deformations were measured by applying a known load uniformly over the surface (in the form of heavy steel nuts) and observing the deflections. This information was needed also so that the wind-induced deflections could be calculated. The results of these calculations show that the effect of an 18 miles per hour wind in deflecting the surface plates adds an RMS value of 0.0006 inch (0.015 mm) to the total telescope surface error budget.

(v) Effects of temperature differences on the surface plates were measured. These are described later in Chapter III, Section 4(c).

This design of surface plate appears to be entirely satisfactory. The fabrication costs have been studied. The actual fabrication procedure prior to surface adjustment does not require very close manufacturing tolerances, since the final accuracy is achieved by adjustment. The measuring technique used at NRAO would certainly not be used for setting and testing in a fabricating shop; quite simple automatic direct reading devices can be used to measure the surface contours. Such techniques are well-known in industry. At NRAO, six man-hours were required to adjust and test one surface plate. Even if this were required in quantity production, the cost per square foot of surface would not be excessive. Each plate is about 12.5 sq. feet of surface and weighs about 50 pounds.

As a final note, it is interesting that both the precise 22-meter (72 feet) antennas built in the USSR use a very similar method of setting the surface. The newer antenna, in the Crimea, has about 40,000 screw adjustments operating on its surface, and (see Table 18) achieves an RMS surface accuracy of 0.005 inches (0.12 mm).

(d) Alternative techniques for fabricating surface plates. Despite the success of the NRAO-designed surface plate, the search has continued for other possible means of fabricating the surface. The search was partly prompted by the continued improvement in fabrication techniques and machines used for a variety of tasks in making precisely shaped objects. The aerospace industries have had to meet difficult challenges in making parts for high-performance aircraft and for launch and space vehicles. Large digitally-controlled machines which can shape surfaces in three dimensions are quite common. Techniques of stretch-forming metal sheets, producing bonded metal honeycomb material or mold-forming materials such as fiberglass, are continually being improved. It was therefore desirable and prudent to investigate various other techniques, particularly those which exist in industry, to find what alternative methods for surface-plate fabrication exist.

Accordingly, studies have been carried out under contracts with the Western Development Laboratory Division of Philco-Ford Corporation and the Rohr Corporation to investigate a variety of other possible fabrication techniques. Reports resulting from these contracts are in the Appendices. We will therefore list the fabrication techniques which have been considered and then describe briefly one of the most promising.

The two studies covered the following possible techniques:

(i) The NRAO design already described.

(ii) A stretch-formed aluminum skin is attached to a conventional welded aluminum support framework. The skin is thick enough so that the surface (which is within about 1 mm of the correct shape) can be machined to the required tolerance, using a numerically-controlled (N/C) machine tool.

(iii) An aluminum support frame is fabricated and the upper surfaces of its ribs are machined, using N/C, to the required accuracy. A stretch-formed aluminum sheet is then attached to these ribs.

(iv) A mold of the required shape to be used as a master pattern is made by using centrifugal force applied to a quick-setting plastic material. (A process of this kind was used some years ago to make small reflectors.) From such a mold fiberglass surface plates with sprayed metal for reflection are produced. An alternative to this technique is to make the molds on an accurate N/C machine.

(v) A conventional surface plate and support structure is resurfaced with a thin layer of metal-sprayed fiberglass. The metallized fiberglass surface comes from and has the accuracy of a precisely made mold. The requisite strength comes from the aluminum support structure.

(vi) The surface plate is fabricated complete from bonded-aluminum honeycomb material.

(vii) A complete surface plate and support structure is cast from a suitable type of aluminum (A356-T61 for example). The surface is machined to shape on N/C machines.

The studies have shown that several of these techniques are possible; one of the most promising when all factors, particularly cost, are considered is (vii). We therefore describe this in more detail.

(e) The machined-contour surface plate (Philco-Ford WDL Division Report). The first step in this process is to make a casting in aluminum of the entire surface plate and support structure. A typical structure is in Figure 11, where the stiffening ribs below the surface are shown. Such a casting can be made in a sand mold; the costs are not high and adequate dimensional accuracy (for this first step) can be achieved. The technique is widely used; it results in a structure which high stability for machining and good rigidity. A material such as A356-T61 has excellent characteristics for casting and a yield strength of about 30,000 psi. Dimensional tolerances from the cast run about ± 0.030 inches (± 0.76 mm) and the surface roughness is about 300 micro-inches.

The surface is then machined to the required contour on N/C skin mills. These work to within 0.0005 inch (0.013 mm) of the data recorded on tape and are capable of meeting the required surface tolerance of the plate. They are much used in the aerospace industry; for example, the Boeing Corporation operates machines with work tables 130 feet in length; these machines could work two surface plates at a time.

More esoteric machining methods are used in the industry; electrochemical, electrical discharge or chemical are some examples, but the N/C machines meet the task at not-too-great cost.

(f) Setting the plates on the telescope.

(i) Methods of measuring the surface. The surfaces of large reflector antennas have been measured and set in a variety of ways; for a recent survey see Findlay (1971). Small antennas for millimeter waves have been measured using the machines with which the surface was made, but such methods are not available for dishes of more than about 10 meters in diameter.

Larger antennas must be surveyed after they are built. Such surveys are usually first made with the antenna pointed to the zenith and the methods so far used fall into three classes. Figure 12 shows the principle of these methods.

The most commonly used (the "range-angle" method) has been to measure the angle $\theta$, using a theodolite T placed a distance h above the vertex of the dish. The line VF may be established by sighting on F or, more usually, $\theta$ is measured by reference to the local gravity vertical. Then, either the distance VP or the distance from V to P along the dish surface is measured with a surveyor's tape. It should be noted in this and in the methods that follow, V and F need not be the exact positions of the reflector vertex and focus, since enough targets are measured to solve, eventually, for the departures in position of the targets from the best-fit parabolic surface and also for the positions of the focal

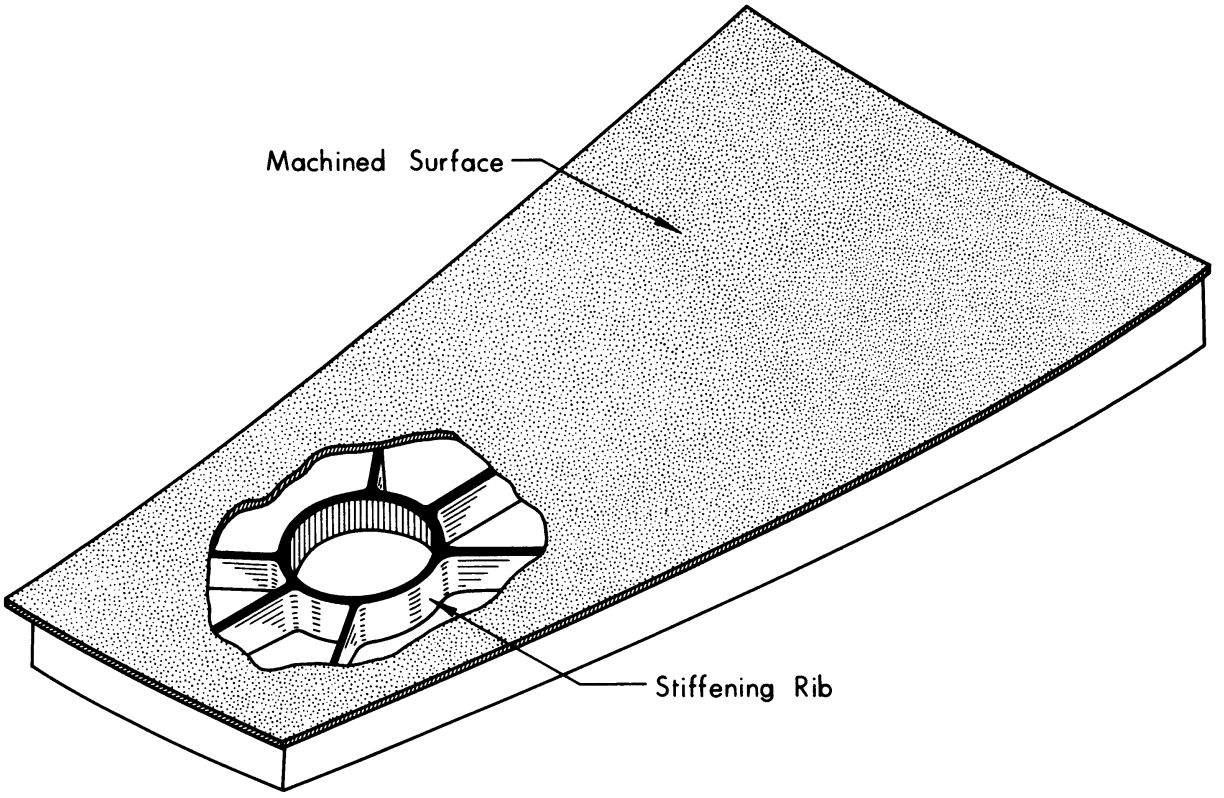


Figure 11. The machined contour surface plate.

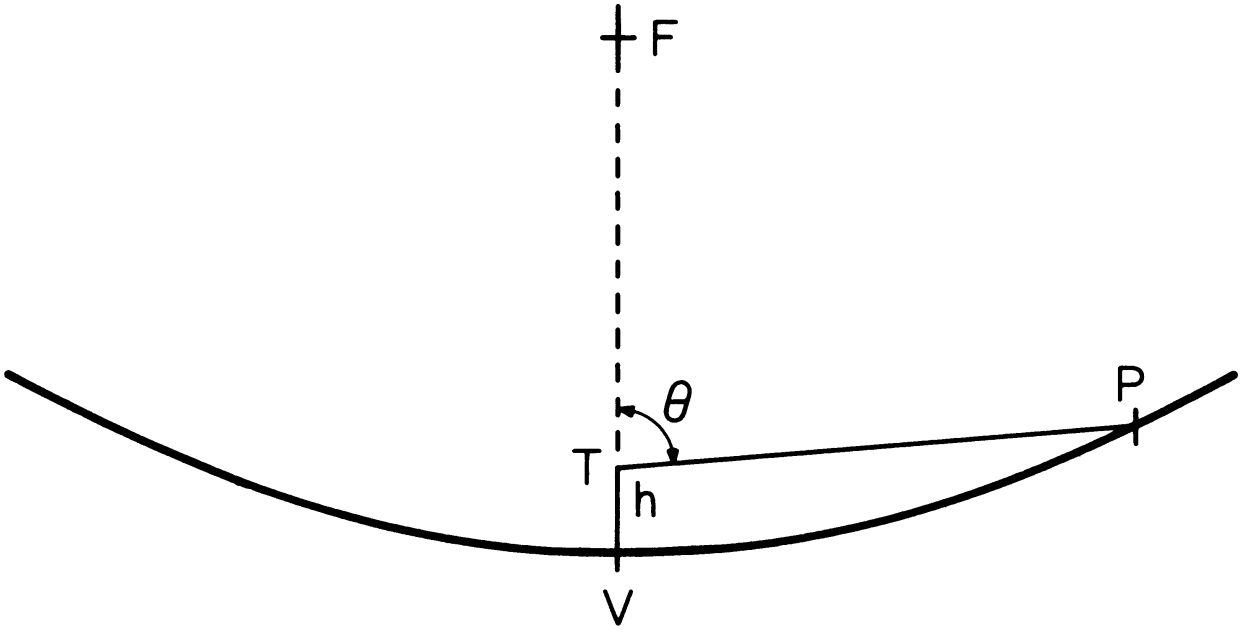


Figure 12. Measurements of the antenna surface.

point and vertex of this paraboloid with respect to the chosen position of V. This technique has been widely used, and at NRAO, for example, using a good theodolite and a contour drilling tape, a measurement accuracy of ± 0.01 inches (± 0.25 mm) has been achieved on the 140-foot reflector.

Another method has been to use two angle measures, one made from T at h and one at a greater height h'. The difference (h'-h) is accurately measured and the range TP deduced. This may be called the "range-finder" method, and it has not been found to be as good as the first.

The third method which only measures distances (the "range-only" technique) measures VP and FP with precise ranging techniques, usually using modulated light-beam range-finders. It has been tested and shows promise (Findlay 1971).

(ii) The methods proposed for the 65-meter telescope. The surface of the telescope will be set by one or both of two methods; the first is an improvement of the range-angle method and the second is a range-only technique. As with all reflector telescopes, the final tests will be the measurement of the gain (aperture efficiency) of the reflector at short wavelengths. This measurement confirms the reflector accuracy, but cannot in its simplest form give information on how to correct the surface adjustments*.

(iii) Surface setting by range-angle methods. The first stage in setting the surface plates will start when the reflector structure is complete and the panel structures are mounted. (These are the space frames, about 30 feet in linear size, on which the surface plates are to be mounted.) The reflector will be pointing to the zenith at this stage. The 60 homologous points on the 44 panels (refer to Figure 7) will be measured by the range-angle method. This can be done using a tape and theodolite, since an accuracy of about one or two millimeters is required. This measurement is intended mainly to confirm that the structure is geometrically capable of accepting the surface plates and that sufficient adjustment range will be available on each plate. It will also be used, however, to make rough settings of the adjustment jacks for each surface plate, so that when they are erected the surface should be within perhaps two or three millimeters of its required position.

After all surface plates are mounted, targets suitable for range-angle measurements will be mounted on the plates. These targets will be similar to those used at NRAO for 140-foot telescope measurements. They fit into holes drilled into the surface plates; these holes are drilled

---

* B. G. Clark has suggested using an extension of this technique which will allow the reflector errors to be corrected. It involves measuring the amplitude and phase of a wave reflected by the dish from a point source--in principle it can measure the reflector profile.

using a contour drilling tape laid on the reflector surface, so that the distances of each ring of targets from a central reference point (V in Figure 12) is known. A sketch of a typical 140-foot target is shown in Figure 13; for the 65-meter telescope the reference dots on the target will be replaced by thin engraved lines. One target will be mounted on each one of the surface plates at each corner where four surface plates come together. We deal later with the method by which all four corners are adjusted to this one target.

At this stage the telescope surface has 18 rings and a total of 3168 targets. The range-angle method is next used in a refined form to measure the target positions. The angle measure is made by using the Zeiss pentaprism system (Kühne* 1966). In principle it replaces the theodolite in the conventional method with a quartz pentaprism, a separate pentaprism being used for every elevation angle to be measured. Figure 14 shows the system. The pentaprism is mounted on a rotating table, the axis of which has been optically aligned with the axis of the fixed alignment telescope. This axis becomes the reference axis of the adjusted surface. All targets in a given ring are observed by rotating the prism table. The target face is marked with graduations and the departure of the target position from the angle $\theta$ is measured by reference to these graduations. Readings can be semi-automatic; the prism table rotation can be programmed. It is not necessary that the prisms be manufactured to precise values of $\theta$ (which would be very expensive) but the value of $\theta$ for each prism must be accurately known. Departures of $\theta$ from the value required are allowed for by making small (known) changes in the distance SV for each prism.

The method has been used on at least two telescopes, the 25-meter dish at Raisting and the 34-meter dish at Werthoven. In neither case was our standard of accuracy needed, but it seems reasonable that the method can have the following measurement accuracy:

Measurement of distance along the surface from V to P—
1 part in 125,000 plus a constant error of $\pm$ 0.2 mm.

Measurement of $\theta$, including errors of measuring the pentaprisms—$\pm$ 0.75 arc seconds.

Kühne's paper gives an expression for the RMS error $m_n$ of the position of P measured along the dish normal n (Figure 14)

---

* We are happy to acknowledge the assistance of Mr. Kühne in providing further information about the pentaprism system.

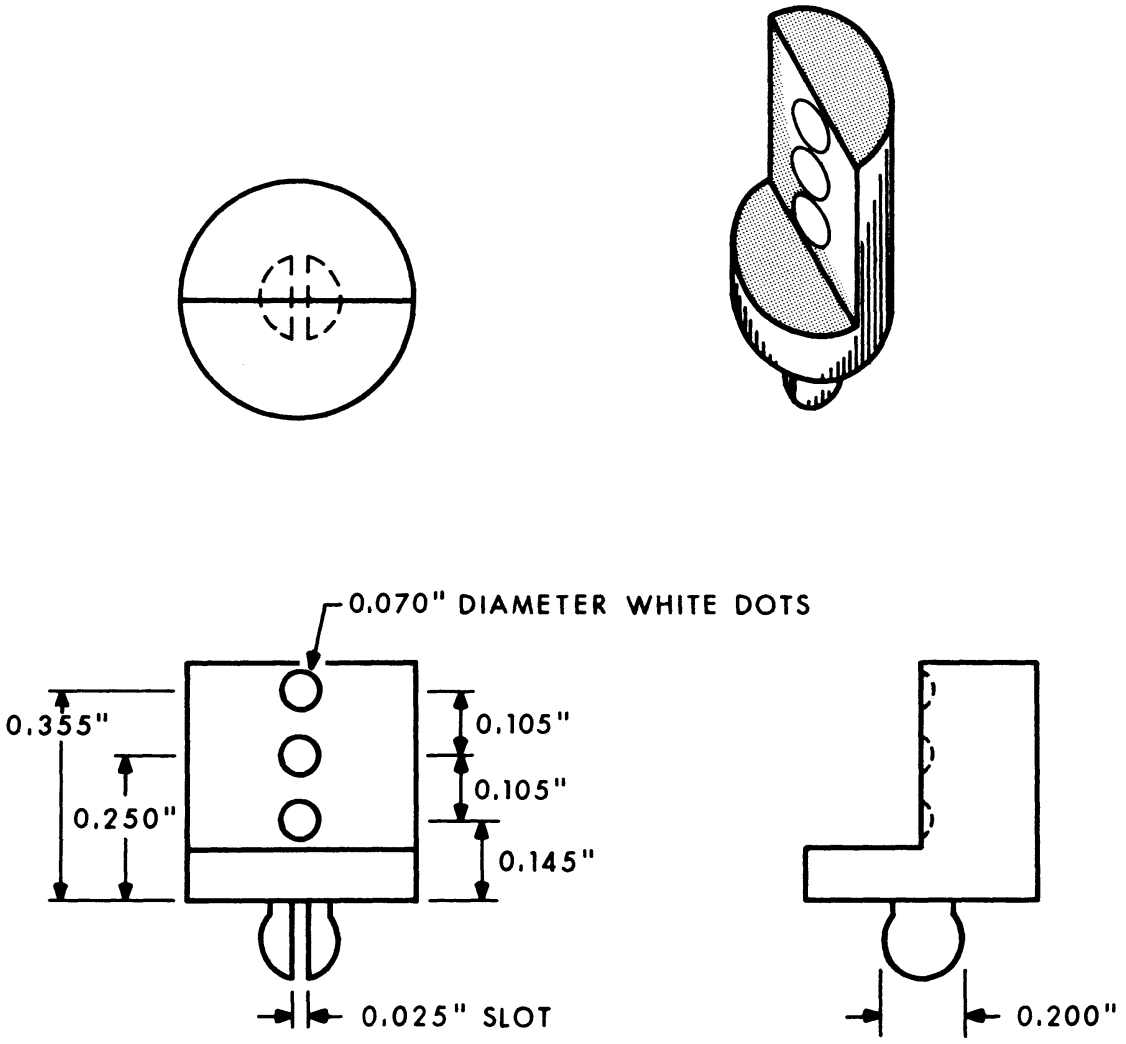


NOT TO SCALE

Figure 13. The targets used for measuring the surface of the 140-foot telescope.

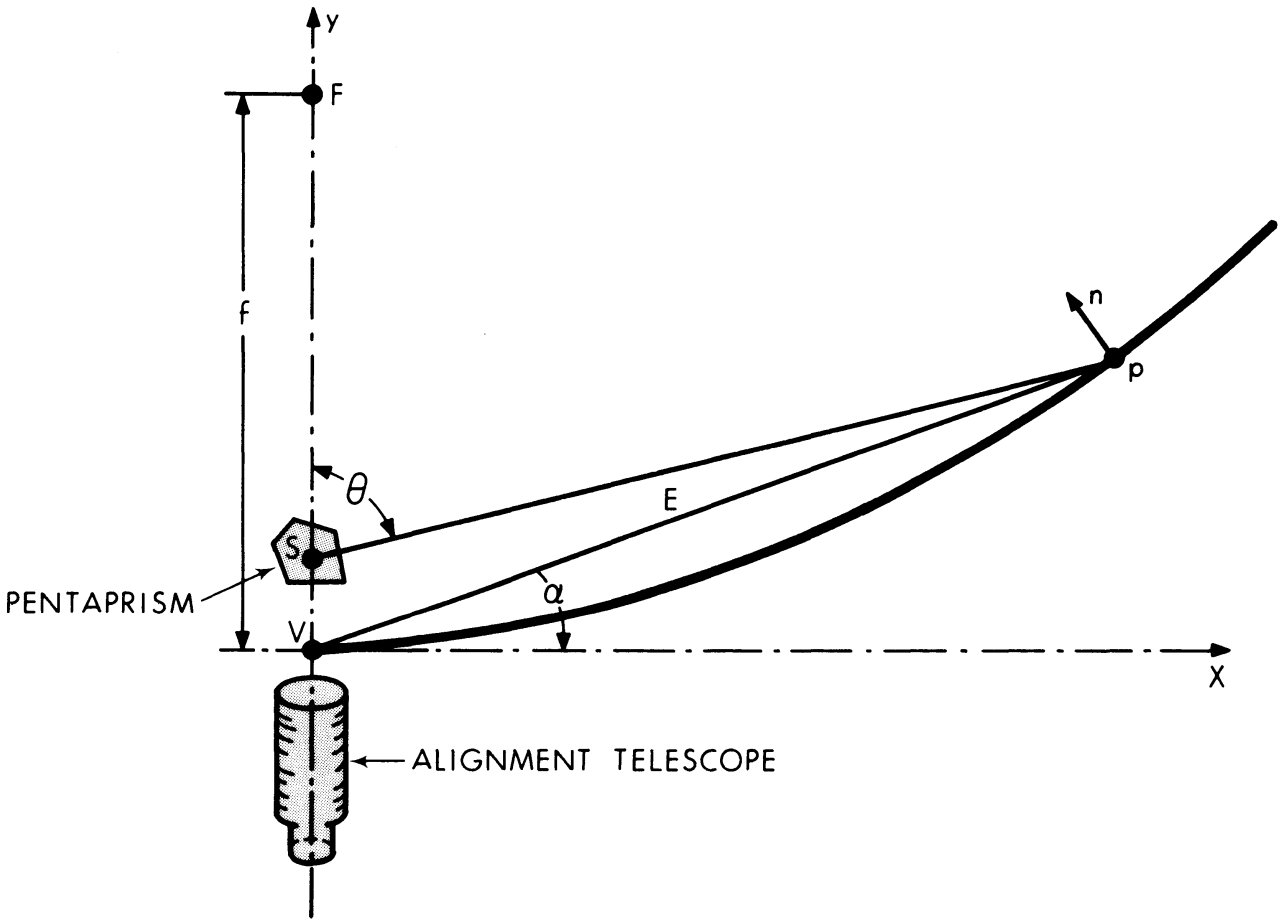


Figure 14. The use of a pentaprism to measure the antenna surface.

$$m_n = E\left\{\left(\frac{m_e}{4f}\right)^2 + m_\alpha^2\right\}^{1/2} \qquad \text{II(1)}$$

where $m_e$ is the RMS error in measuring VP (= E) and $m_\alpha$ is the angular RMS error.

$$\left.\begin{aligned} \text{If we take } m_e &= 0.2 + 8\text{x}10^{-6}\ E\ (m_e \text{ and } E \text{ both in mm}) \\ m_\alpha &= 0.75 \text{ arc seconds } (3.64\text{x}10^{-6} \text{ radians}) \end{aligned}\right\} \qquad \text{II(2)}$$

and apply II(1) to our 18 target rings, we get the following Table 6.

Table 6. Measurement Errors in the Pentaprism Method

| Target Ring | No. of Targets | E in Meters | RMS Error $m_n$ in mm |
|---|---|---|---|
| 1 | 32 | 3.3 | 0.0138 |
| 2 | 64 | 4.8 | 0.0204 |
| 3 | 64 | 6.4 | 0.0275 |
| 4 | 64 | 7.9 | 0.0345 |
| 5 | 128 | 9.4 | 0.0416 |
| 6 | 128 | 11.4 | 0.0514 |
| 7 | 128 | 13.3 | 0.0611 |
| 8 | 128 | 15.2 | 0.0711 |
| 9 | 128 | 17.2 | 0.0821 |
| 10 | 256 | 19.0 | 0.0922 |
| 11 | 256 | 20.9 | 0.1032 |
| 12 | 256 | 22.7 | 0.1140 |
| 13 | 256 | 24.5 | 0.1258 |
| 14 | 256 | 26.3 | 0.1375 |
| 15 | 256 | 28.1 | 0.1497 |
| 16 | 256 | 30.1 | 0.1635 |
| 17 | 256 | 32.0 | 0.1775 |
| 18 | 256 | 33.9 | 0.1913 |

Note that there is one more target ring than the 17 rings of plates shown in Table 5. This is due to the fact that target rings occur on the inside edge of the plate ring No. 1 and the outside edge of plate ring No. 17.

From the last column we derive the 1σ value of the RMS measurement error when all 3168 targets are measured with their associated RMS errors ($m_n$)

$$\text{RMS measurement accuracy} = \left\{ \frac{1}{3168} \sum_i n_i m_{ni}^2 \right\}^{1/2} \qquad \text{II(3)}$$

$$= \pm\ 0.125 \text{ mm } (0.0049 \text{ inches})$$

The range-angle method thus seems able to achieve the requisite measurement accuracy. A few practical comments should be made, however. First, at each target we have to adjust the corners of four plates to the single target. This can be done by a simple jig which by reference to gravity using a spirit level carries the required elevation from the one target to the four corners. Second, it will not be possible to measure all the targets in one night. The measurement time per target will be about 30 seconds, so that on one night only a few hundred targets can be measured. Thus the setting process will be referenced on each night's measurement to targets on the plates above the 60 homologous points, and blocks of other targets will be measured with respect to these master targets.

(iv) Setting the surface by range-only methods. A method has been developed by which the surface can be surveyed and adjusted by measuring the distances TP and FP (Figure 12). T is now to be regarded as a fixed reference point near the vertex of the dish, and F is a fixed point near the focal point. The method uses a modulated light-beam distance measuring equipment mounted near V. The distance from the instrument reference plane to P via a mirror at T is one measurement; T is then removed and the distance from the instrument to P via a mirror at F is measured. To discuss the practicality and accuracy, we first consider the properties of distance-measuring systems for the task. It is clear that an accuracy of about 0.1 mm (0.004 inch) is required to achieve our goals. The requirement is less strict for the measure of TP, but is approximately the same for all targets in the measurement of FP.

Modulated light-beam distance measuring systems have been used in surveying for about 20 years, but they have mainly been designed for use over distances of several miles. Their use is described, for example, in the book by Saastamoinen (1967) where the Geodimeter and Tellurometer are discussed in detail. Two instruments made by Zeiss (Leitz 1969) and the Mekometer II (Froome and Bradsell 1966) are also of interest in showing the accuracy of the techniques and the ease with which the instruments can be made to read out automatically in digital form.

The principle involved is simple. A high intensity light beam is amplitude modulated at a frequency which can be a few MHz up to about 500 MHz. This beam is sent over the long path to be measured and

also over a short reference path. Figure 15 illustrates the method. The two returned light signals fall on photodetectors; the two outputs of which are identical waveforms at the modulation frequency f. The phase difference between these waveforms is accurately measured, usually by mixing each with the same local oscillator to give waveforms at the chosen intermediate frequency. The difference (L) in the one-way lengths of the long and short paths can be written

$$L = \frac{1}{2}(n + \varepsilon)\lambda \qquad \text{II(4)}$$

where $\lambda$ is the wavelength in air of the modulation frequency f, n is an integer and $\varepsilon$ a fraction less than unity. As an example, suppose f is 500 MHz, $\lambda$ = 60 cm and for a measurement where L is already known to a few centimeters, n is known. The phase difference between the two waveforms measures $\varepsilon$; good electronic techniques allow a measurement accuracy of $\varepsilon$ to about 2 in $10^4$, so that L is known to $\pm$ 0.06 mm. Small corrections for the refractive index of air can easily be made when this sort of accuracy is required over paths of up to 100 meters in length. The system is thus capable of making range-only measurements on the telescope to our required accuracy.

The method proposed is to measure with such an instrument mounted near the dish vertex V (Figure 12) the path lengths VTP and VFP. Rotatating tiltable mirrors mounted at T and F allow of these paths being followed to all targets. The targets themselves have reflecting faces to return the TP and FP rays along their own paths. The range indications and target identifications are produced in digital form and stored on tape.

The mirror at F will only be as stable in position as the feed support allows. Measurements will be made in low wind conditions, thus F moves only because of slow temperature effects in the feed legs. Readings of groups of targets are taken in blocks of 20-50 (in a total time of about 10 minutes) and each block of readings permits a solution for the target errors and for the position of F. Thus slow movements of F can be eliminated from the measurements.

A 550-MHz distance-measuring instrument has been built and tested at NRAO. It has the required stability and accuracy; its output is digital in steps of 0.01 mm. This is achieved by the correct choice of modulation and digit frequencies. Figure 16 is a block diagram of the instrument.

This method has been developed as an alternative or a possible improvement over the range-angle system already described.

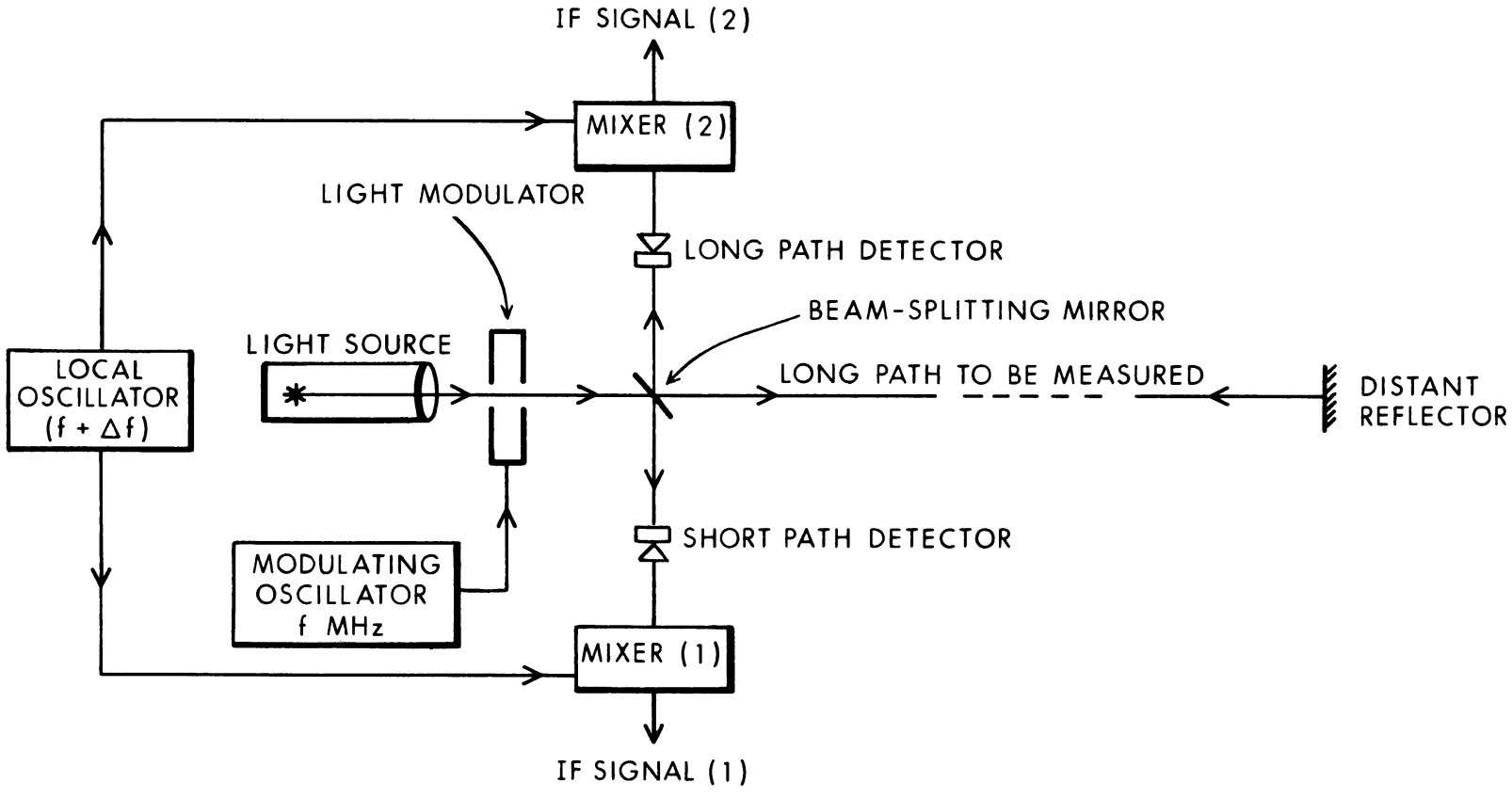


Figure 15. The modulated light beam technique for distance measuring.

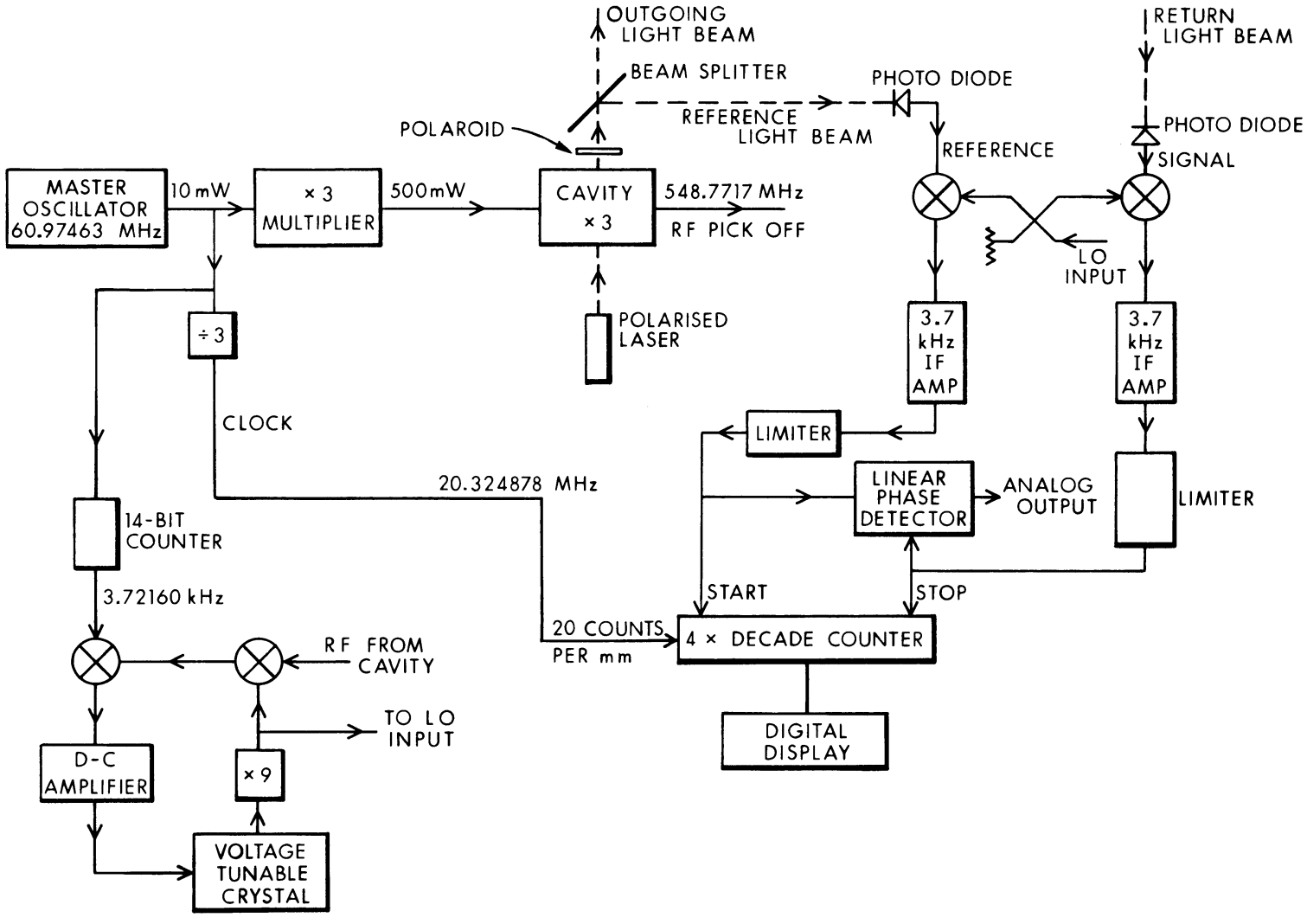


Figure 16. The NRAO modulated light beam system.

6. The Cassegrain System, the Feed Support, and the Observing Rooms

(a) The Cassegrain system (S. von Hoerner Report No. 31). The various considerations on which the choice of the parameters of the Cassegrain optical system depend are covered in the above-referenced report. We can summarize them as follows:

(i) The telescope will be used at longer wavelengths as a prime focus instrument, and at shorter wavelengths as a Cassegrain. The choice of the approximate wavelength at which the change takes place affects the choice of subreflector size, the design of the vertex mounted feeds, and these factors in turn are linked with mechanical designs of the instrument cabins and subreflector mount.

(ii) The homologous behavior of the main reflector carries with it the fact that the primary focal length of this reflector changes with the telescope's elevation angle. Also, the reflector axis of symmetry moves somewhat, as the elevation axis changes, with respect to the line joining the vertex of the reflector to the center of the apex of the feed support system. These motions require appropriate movements of the subreflector and feeds to be possible and the requirements for such motions affect the choice of the Cassegrain geometry.

(iii) In the Cassegrain mode, various types of beam switching and beam movement may be required for different observing programs. The telescope beam may be moved by tilting the subreflector so that if more than one feed is placed near the secondary focus the telescope can switch easily from one observing system to another. Periodic tilting or nutating of the subreflector can allow of various "on-off" observing programs which are used to reduce the effects of sky noise. The ability to perform these various beam movements depends on the size and inertia of the subreflector and so affects the choice of Cassegrain geometry.

(iv) The primary reflector focal length was fixed at the focal length/diameter (f/D) ratio of 0.426 since this value is standard for all the larger NRAO telescopes. Thus, any front-end equipment used on the Green Bank telescopes will be interchangeable with the 65-meter telescope. This primary f/D ratio does not harm the Cassegrain performance of the 65-meter instrument, but thought has to be given to the dimensions of the feed horns likely to be used at the secondary focus. This again affects the choice of Cassegrain geometry.

(v) The effective aperture of the whole telescope is blocked by the subreflector and its support structure. The amount of this blocking which can be tolerated must be considered in the choice of geometry.

We will not follow through the method by which a suitable Cassegrain geometry was selected, but will only give the description and characteristics of the system proposed. Figure 17 shows the geometrical optics of the system. Parallel rays from infinity pass through the prime focus of the main reflector in the prime focus mode; in the Cassegrain

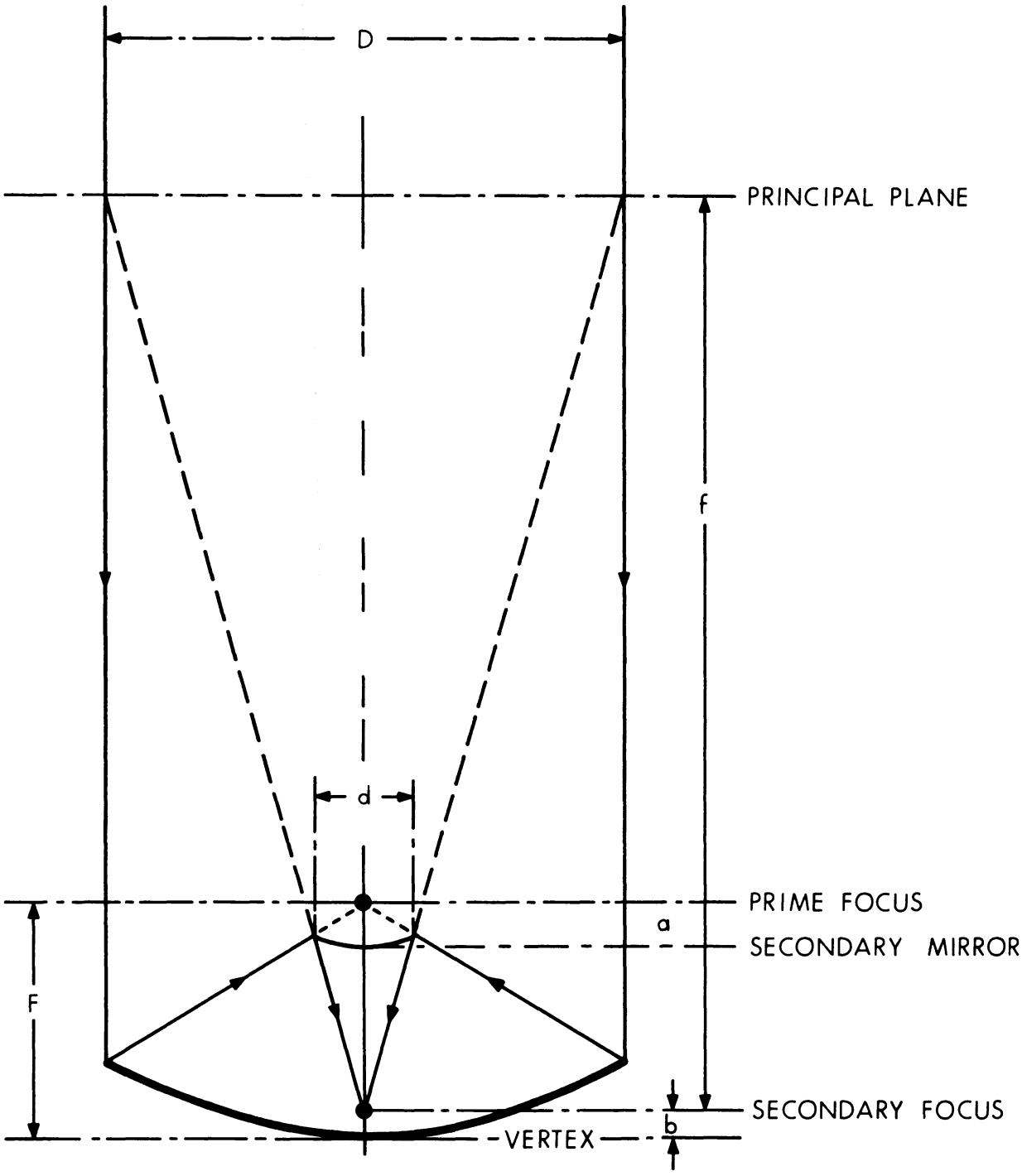


Figure 17. The geometrical optics of the Cassegrain system.

mode they are reflected to pass through the secondary focus. The primary focal length F is the distance from the primary focus to the main reflector vertex while the secondary focal length f is the distance from the secondary focus to the principal plane of the system. Thus the Cassegrain system can be considered to be a reflector of diameter D and a focal length f which is considerably longer than F. The ratio f/F is referred to as the magnification of the system. (Note that Figure 17 is not to scale, and is oversimplified--with such wide-angle optics principal planes become curves.)

The following Table 7 summarizes the dimensions and performance of the Cassegrain system.

Table 7. The Cassegrain System

| Property | Value |
|---|---|
| Main reflector diameter (D) | 65.0 m (213.1 feet) |
| Main reflector focal length (F) | 27.70 m (90.88 feet) |
| Subreflector diameter (d) | 3.657 m (12.00 feet) |
| Secondary focal length (f) | 437.46 m (1435.3 feet) |
| Magnification (f/F) or (M) | 15.793 |
| Longest wavelength (lowest frequency) for use as Cassegrain | About 4 cm (7.5 GHz) |
| Height of secondary focus above vertex of main reflector | 1.524 m (5.00 feet) |
| Distance from prime focus to vertex of subreflector (a) | 1.559 m (5.11 feet) |
| Approximate lengths and aperture widths of secondary feed horns at wavelengths of 3.5 mm and 3 cm | $\lambda$ — Horn Length — Horn Aperture<br>3.5 mm — 34 cm — 5.3 cm<br>3.0 cm — 2.9 m — 46 cm |
| Lateral displacement of feed from secondary focus which is permissible before either the coma becomes objectionable or the spillover limits gain and increases noise seriously | $\lambda$ = 3.5 mm — about 115 cm (3.75 feet)<br>$\lambda$ = 3 cm — about 2 m (6.6 feet) |

The table demonstrates some of the advantages gained from the use of a Cassegrain with a magnification of about 15. The sizes of the feeds at the secondary focus are not unreasonable, yet quite large feed displacements from the vertex (as would be used, for example, if multiple feeds were used) are quite possible. In fact, the number of feeds which can be used for mapping and for short-wavelength surveys will most probably be limited by the cost and complexity of the radiometers and not by the radio telescope.

Finally, the subreflector itself should be considered briefly. It is a hyperboloid, with a focal length (focus to vertex) of 1.559 m (5.11 feet). The surface accuracy must be high; reflectors of this size can be fabricated with RMS surface errors of somewhat less than ± 0.002 inches (± 0.05 mm) and this is the planned accuracy of the reflector. Its weight will be kept low to allow of its being moved rapidly in the modes needed for beam motion.

The subreflector will be mounted in such a way that it can be removed and replaced readily; this allows of rapid change-over between the Cassegrain and prime-focus modes of using the telescope. The mounting allows of a range of controlled movement of ± 1 inch (2.5 cm) in both the axial and lateral directions; it can be tilted and rotated to give a nutating motion. It can be positioned to an accuracy of ± 0.002 inches (± 0.05 mm) in the axial direction and ± 0.01 inches (± 0.25 mm) in lateral directions.

(b) The feed support (W-Y. Wong Report No. 42). The function of the feed support is to carry the prime focus cabin and all the equipment needed for observing with feeds at the prime focus. It also, in the Cassegrain mode, carries the subreflector. Both these tasks require that the feed support be as stable as possible against deformations due to its own weight and due to the dead loads of the equipment near its focus. It must also not deflect due to wind forces by amounts which would impair the pointing precision of the telescope. The effects of temperature differences between the legs of the feed support will also deform the structure; these effects must be calculated and, if possible, reduced to an acceptable value. The structure must, of course, withstand the survival loads due to wind, ice or snow.

The structure that meets these requirements is shown in Figure 18; its design was essentially determined by the need to keep the structural deformations small. It is a tetrapod, each of the four legs passes without interference through the dish surface. (This section is a tubular member to minimize the problem of clearing the neighboring panel structures.) The connection between this tubular member and the built-up leg structure is braced in four directions to the nearest surface support points. This bracing does not affect the dish surface accuracy to any appreciable extent. The four legs are built-up from tubular members (to minimize wind forces) and each leg is guyed at points near its

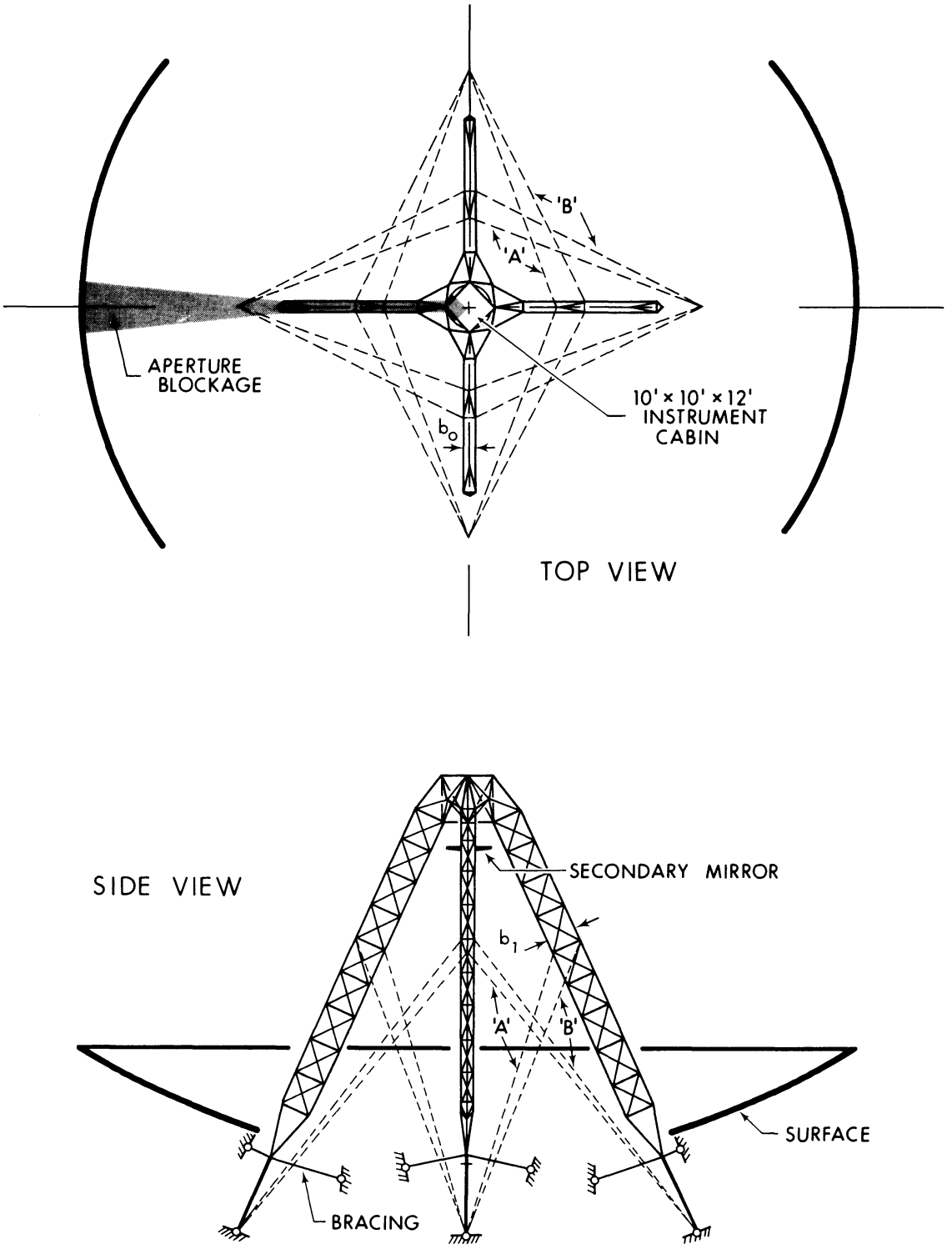


Figure 18. The feed-support structure.

center to increase its lateral stiffness. The guys terminate at the joints in the main reflector structure where the feed legs themselves end. The legs are quite deep structures ($b_1$ in Figure 18 is 2.5 m or 8.2 feet) but their width ($b_o$) has been kept fairly small (1.0 m or 3.3 feet) to reduce their blocking effect on the aperture.

The deflections of the feed support under gravity and wind loads have been calculated. The gravity deflections, when taken together with the movement of the main reflector axis as it deflects with changing elevation angle, are not serious and are, of course, removed from the overall pointing error budget in the calibration process. A steady 18 miles per hour wind deflects the feed support in such a way as to translate and rotate the subreflector. The beam shifts due to these movements have opposite signs; the resulting beam shift is calculated to be 1.08 arc seconds, and this figure is used in the computation of the total pointing and surface error budgets in Chapter III.

The long feed legs are the most sensitive parts of the whole telescope to the existence of temperature differences. Such differences between the legs influence the telescope pointing. For example, if we assume that the temperatures of the four legs lie at random within a temperature range of $\pm$ 1° F, the resultant pointing error is 2.0 arc seconds. This figure is used in the error budgets of Chapter III for the case of operation on a clear night. When the sun shines on the legs the pointing is considerably worse, as the error analysis of Chapter III shows.

The dynamical behavior of the feed support, with the loads of the observing cabin and subreflector, have been studied and a natural frequency at 4.2 Hz is found for oscillations about an axis parallel to the reflector axis. This is satisfactory.

The feed support and observing cabin give a total aperture blockage of 6.4 percent. This figure does not include the small effects of the guy cables, but it is quite acceptable.

The feed support is designed to be fabricated from the same type of steel used for the reflector and tower structure.

(c) The observing rooms. The telescope has observing rooms located at both the prime and the secondary focal points. Each is 10 feet square with a length of 12 feet. These rooms house the feed horns and front-end electronic equipment; they are insulated and have good temperature control systems. Each can carry about 10 tons of equipment.

The room just behind the prime focus is connected to the apex of the feed-support structure. It is provided with a mount for the standard-sized NRAO front-end boxes; this mount allows of rotation of the whole box about its axis and also permits the feed to be focussed. These movements are remotely controlled. Such mounts have been in use at Green Bank for several years.

The observing cabin at the secondary focus rotates as a whole about the axis of symmetry of the reflector. It extends about 5 feet (1.53 m) above the main reflector surface, so that its front wall lies approximately in the secondary focal plane. Several feeds can be mounted through this front face of the cabin; its 12-foot length is sufficient to accommodate the longest feeds required in the Cassegrain mode, and the telescope beam can be moved from one feed to another by tilting the subreflector. This arrangement, similar in principle to that used at the Goldstone 210-foot antenna, allows of rapid change-over between observing programs.

## 7. The Position Reference System

The purpose of the position reference system is to determine the direction of the telescope beam in the sky by reference to the usual system of astronomical coordinates. This is done in two ways; there is a coarse position system, which is used only to ensure that the telescope can be moved and roughly controlled at all times, and a precision position system which is precise enough to ensure the accurate pointing required for short wavelength observations.

(a) The coarse position system (SDL Report H-10, Chapter 10). This system uses 17-bit* angle encoders, one mounted at the azimuth axis and one at the elevation axis. Both are driven by anti-backlash gears. This is necessary for the azimuth encoder, since the shaft center space is required for the passage of cabling. The elevation axis encoder could be axially mounted, but for uniformity it is made the same as the azimuth system.

(b) The precision position system. It is not easy to determine the position of the radio beam with the high precision required by measuring the angular positions of the telescope axes. The difficulties arise because the whole telescope structure, and in particular the towers, deflects under gravitational and wind loads and is deformed by temperature differences in the structural members. Many of these deflections can be arranged not to influence the pointing accuracy of the instrument if the reference position is chosen to be the point in space where the azimuth and elevation axes intersect.

This position is on the reflector structure, behind the reflector surface. (It is close to joint No. 56 and is often referred to in this way.) In order to measure the two angular coordinates of the telescope beam direction from this point it is necessary to carry a reference from the ground up to the axis intersection. This has been done

---

* One bit corresponds to an angle of 9.89 arc seconds with this encoder.

in three large telescopes already (the instruments at Parkes, Goldstone and Algonquin Park) by building a central tower, shielded from wind or sunlight, from the top of which the direction in space of the reflector axis is determined by an optical system (the master equatorial as it is called).

The present design uses the same principle, but instead of using a central tower the position reference platform is fixed in angular position with respect to the ground by making the platform stay locked in direction to light beams projected onto it from stable light sources on the ground. Figure 19 shows the principle of the method. In practice, the system has been designed to use seven autocollimators firmly mounted around the outside of the azimuth track. (Drawing 111-D-011 shows the layout and the autocollimator mounting.) The seven light beams are reflected back to the autocollimators from a seven-sided mirror on the reference platform. The platform itself is supported from the reflector structure, but the mirror is free to rotate about two perpendicular axes (azimuth and elevation) with respect to the structure. The mirror assembly is driven about these two axes by torque motors and the angular positions of the mirror axis with respect to the telescope structure are measured with 22-bit angle encoders which give a resolution of 0.31 arc seconds. The seven-sided mirror is driven by the torque motors, using error signals from the autocollimators to control the servo-loop, so that the mirror faces remain normal to the light beams no matter where the telescope points.

The foregoing general description should be sufficient to describe the principles by which the precision position system works. Since the whole system is so vital to the performance of the telescope, it has been designed in detail and considerable care has been taken to estimate the probable accuracy of position measurement. In what follows the various parts of the reference platform system are described in more detail.

(c) The autocollimators (SDL Report H-10, Section 10.4). Each collimator must meet the following requirements:

(i) It must be capable of sensing simultaneously in both azimuth and elevation and misalignment of the light reflected from its mirror, as compared to the light projected onto the mirror.

(ii) It must operate in full daylight and at night over the required distance (about 200 feet) with adequate precision.

(iii) It must give error indications over an adequate range of misalignment angles and the error indications should be reasonably linear with angle over the angular range near perfect beam alignment.

(iv) It must sense the intensity of the reflected light so that when a light path becomes obstructed, information from the corresponding autocollimator can be rejected.

The D696 special two axis autocollimator made by Davidson Optronics meets these needs almost completely. Its range of daylight operation is somewhat smaller than is ideal, but this can be increased without much difficulty. The two axes use different wavelength light sources in the form of mercury and neon lamps. The instrument is sensitive to angular misalignments of 0.1 arc seconds and, among other outputs, it gives an error signal which is linear over a $\pm$ 27 arc seconds range of angular error of the mirror being referenced.

Seven such instruments will be mounted on strong supports around the telescope. Error signals from two autocollimators are sufficient to control the stable platform, but seven are needed since the light beams are, from time to time, obstructed by the tower and dish members of the telescope. The autocollimators are in temperature controlled enclosures; the possibility that their foundations may move due to long-term settlement or to more rapid heaving of the ground as the telescope rotates is allowed for by mounting a precise tilt-sensor on each autocollimator.

The effects of the atmosphere on the angular stability of the light path from the autocollimator to the mirror have been carefully studied. A single-axis autocollimator was used in a test at Green Bank lasting several months. The light path used was 185 feet long; one end was at ground level and the other was about 45 feet above ground on the upper deck of the 140-foot telescope foundation. The path was thus about the right length but at a lower elevation angle (about 14°) compared to the 31° angle the final system will use (see Figure 19). Fluctuations in this lower-angle path can be expected to be greater than in a path of the same length at a higher elevation angle.

The light from the autocollimator was reflected from a mirror whose direction was controlled by a servo loop deriving its error signal from the autocollimator. The characteristics of this servo loop were very similar to those of the servo designed for use with the stable platform.

Thus the test showed the stability of the atmosphere optical path, but it also tested the servo design. The movements of the mirror and the autocollimator error signals could be separately measured to confirm the performance. Means were provided by adding angular disturbances to the mirror shaft, to simulate the effects of disturbances to the reference platform. The atmospheric effects were recorded in the form of measurements of the angular fluctuations of the optical beam. The recording system also derived the RMS fluctuations, and for part of the observations an autocorrelator was used so that the average power spectrum of the angular fluctuations could be measured. The system is described in more detail in reports by J. Payne (July 21, September 8, and November 29, 1970). Figure 20 shows a short section of a record of the angular fluctuations of the beam, and Figure 21 is a typical power spectrum of the fluctuations.

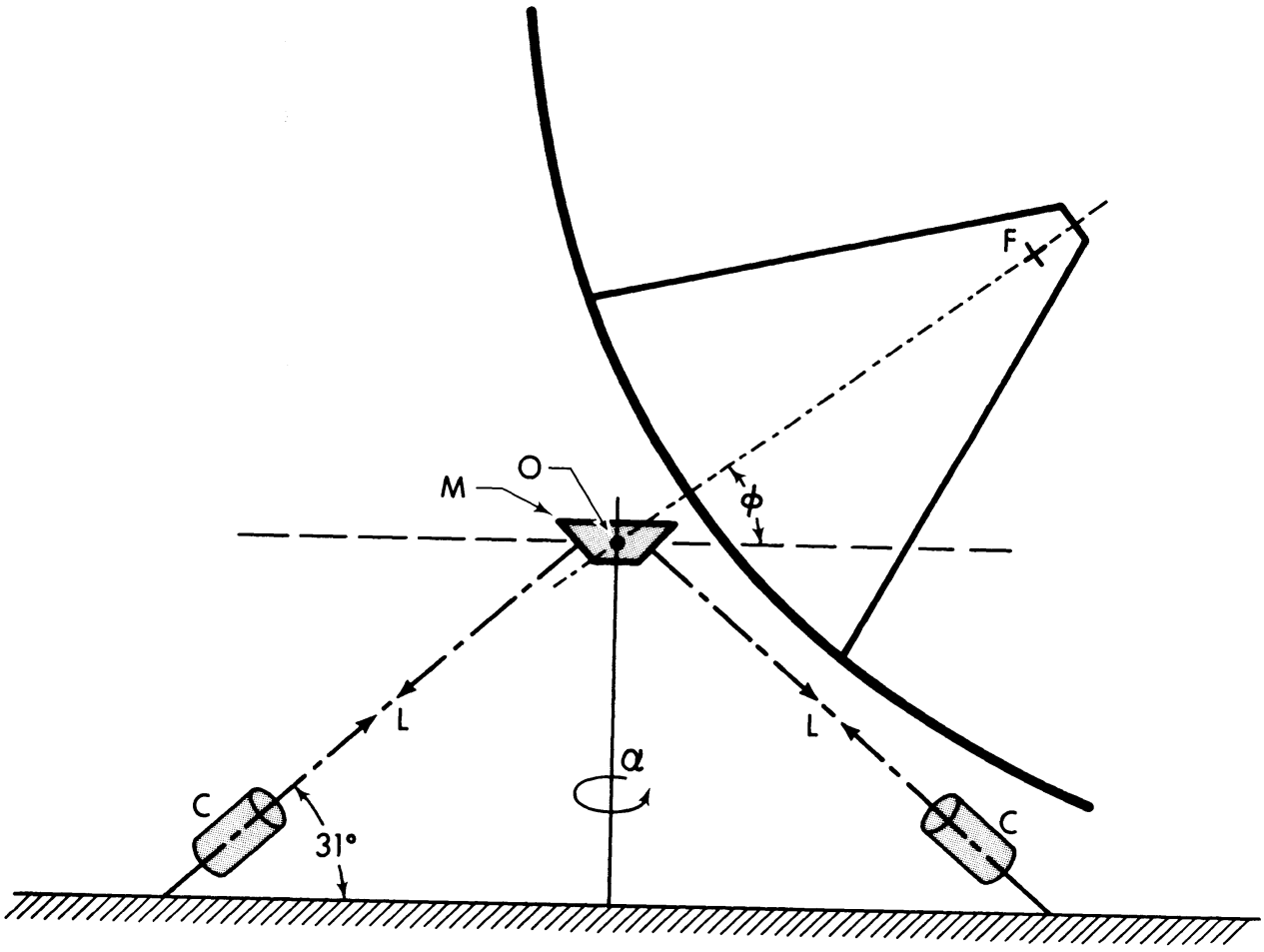


Figure 19. The principle of the stable reference platform.

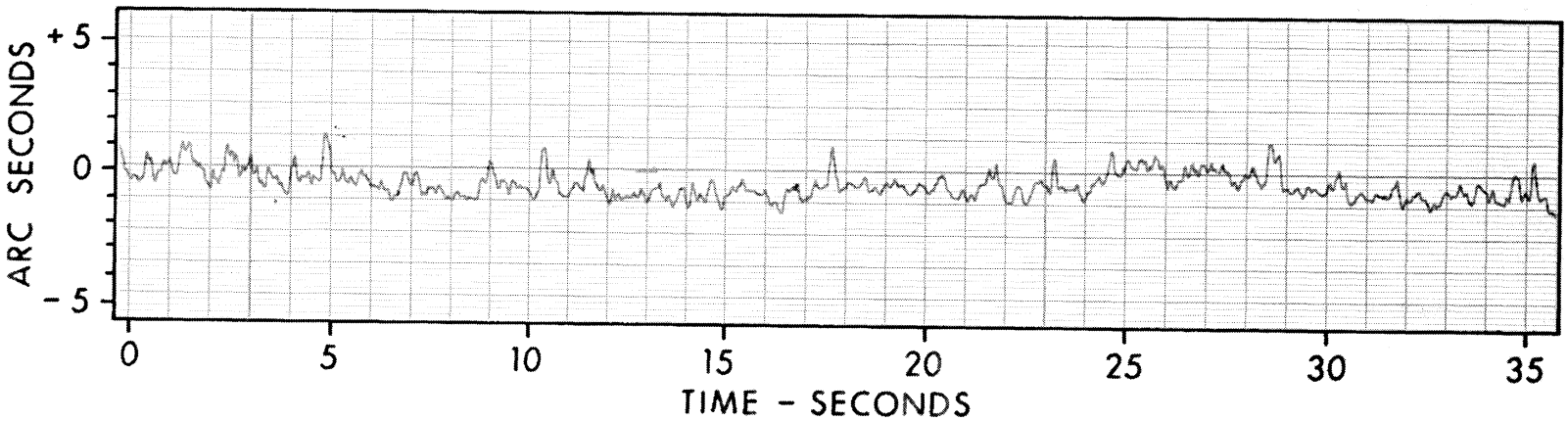


Figure 20. A typical record of the angular fluctuations of the optical path used in the reference platform tests.

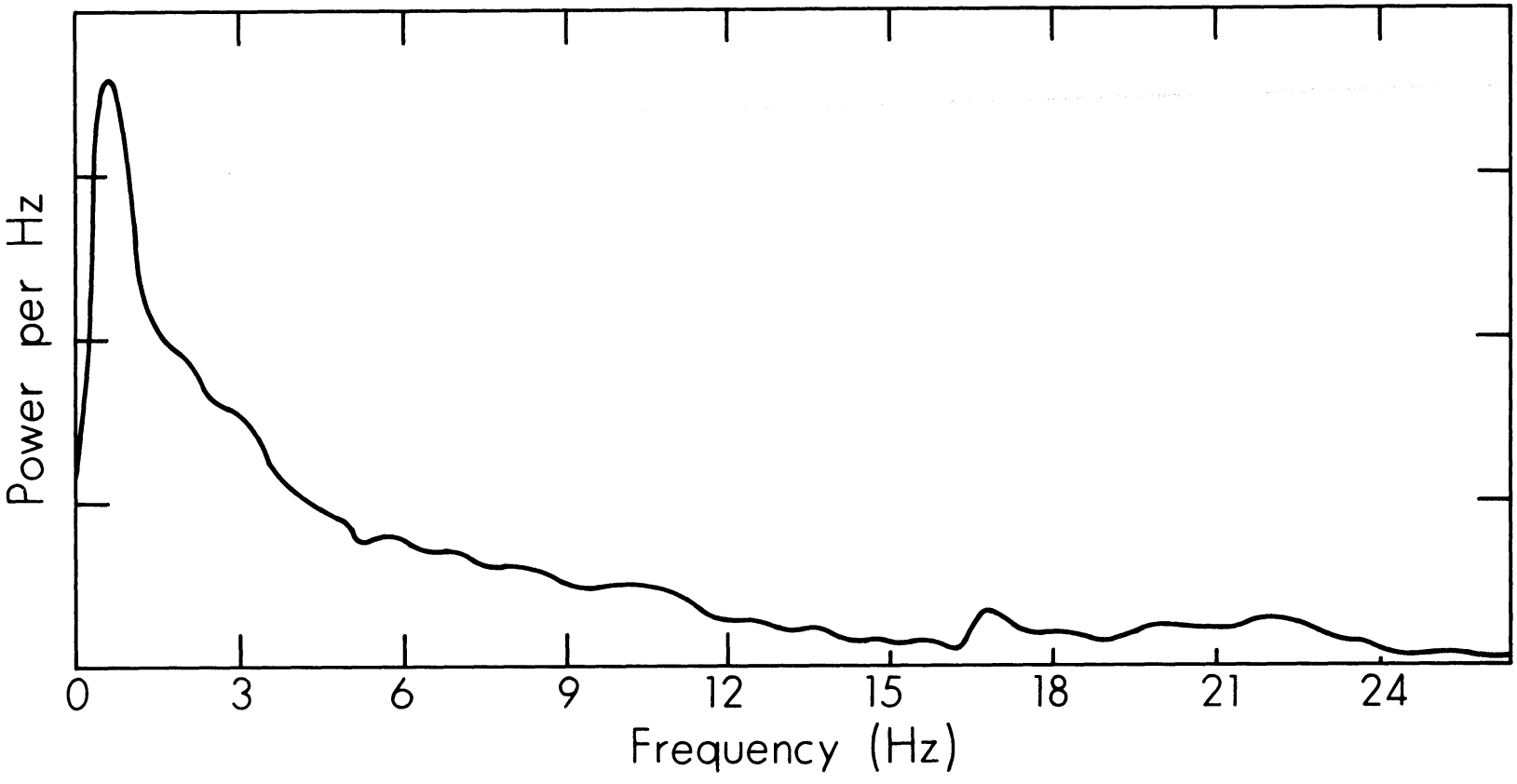


Figure 21. Power spectrum of the angular fluctuations of the optical path used in the reference platform tests.

The results of these tests show that the RMS error introduced into the reference platform servo will be ± 0.60 arc seconds under the atmospheric conditions which for other reasons still permit precise use of the telescope. This value is used in the error budgets of Chapter III.

While the test experiment was in progress, the report of a similar experiment conducted at Marshall Space Flight Center became available (Kurtz and Hayes 1966). They made similar measurements over paths of 3200 meters and 165 meters at elevation angles of 4°. They produced very complete results for the atmospheric effects, which, when allowances are made for the different elevation angles, agree with the NRAO results.

(d) The stable reference platform (SDL Report H-10, Section 10.3). The detailed design is shown in Drawings 111-D-012, Sheets 1-6, and Figure 22 is a general view of the platform. The heart of the system is the seven-sided mirror assembly from which the seven autocollimator light beams are reflected. This is made from a precision machined aluminum casting onto which the seven Pyrex mirrors are bonded.

This mirror assembly is rotated in azimuth and elevation by torque motors; its position with respect to the main telescope member joint No. 56 is referenced by accurate 720-pole inductosyns, and tachometers (to give the velocity component required by the servo) are also shaft mounted. The whole platform operates in a carefully controlled environment and a plastic radome with 12 glass windows covers the mirrors. The light beams enter the radome through these windows, so they are made of precision-ground glass. Two radome designs have been made. In the first, the radome rotates with the azimuth rotation of the telescope; in the second the radome remains fixed with respect to the mirrors. The second design is preferred.

The design of the platform has been developed in detail, both because it is such a vital element and also because it is important to have good knowledge of the inertia of moving parts, friction forces and spring constants for the servo design. The wind forces and moments also have been calculated since these are also needed for the servo design. The details of the thermal control, which keeps all components at (100 ± 1)° F, have been developed. The method of mounting to joint No. 56 has also been devised in some detail and consideration has been given to the way the platform will be aligned on the telescope.

The components required in the platform are all of high-precision, but all are either available or can be made to the required accuracy. The two position encoders are identical, but they deserve special mention. The contribution to the total overall pointing errors of the telescope from the encoders can be kept fairly small, since 22-bit encoders are commercially available. A detailed encoder specification was prepared and sent to possible suppliers. As a result, 720-pole inductosyns (Fecker Systems Division of Ownes-Illinois) were chosen for inclusion in the design. These encoders have been used in other precise systems--

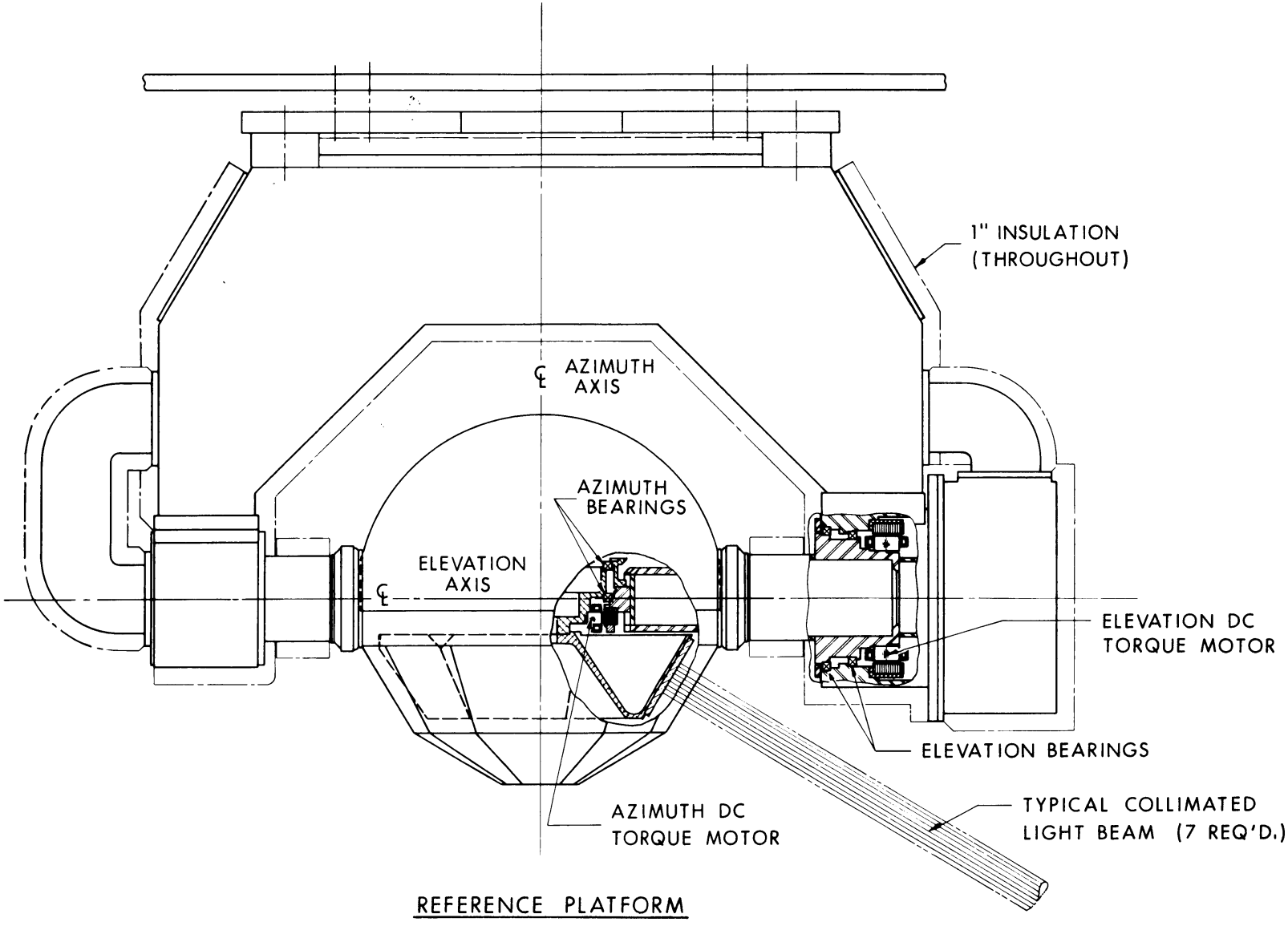


Figure 22. A general view of the stable reference platform.

perhaps the most remarkable being their use by the U. S. Naval Observatory on the 6-inch transit circle.

One further question needs to be considered in the reference platform optics. The motion of the reference point on the telescope structure as the telescope moves is mainly rotation in azimuth and elevation. Nevertheless, small movements of this point in space will occur since it may rise and fall or move laterally as a result of temperature differences in the structure, wind-induced deformations or irregularities in the azimuth track.

These lateral movements have been estimated and the size of the mirrors and collimator beams have been so chosen that the expected movements will not interfere with the performance of the system. The angular accuracy of the system is, of course, not impaired by these small linear translations of joint No. 56.

(e) The platform servo system (SDL Report H-10, Chapter 10.7). In principle, the control of the reference platform to keep the seven-sided mirror held with its axis normal to the autocollimator beams is a straightforward task. However, in practice, there are a number of considerations to be met in order that the full angular accuracy of the system is achieved. For example:

(i) At any time several of the autocollimators will be providing error signals in each of the azimuth and elevation axes. These signals must be averaged before they are used as the input position errors to the platform servo.

(ii) As the telescope structure rotates, some autocollimator beams become obstructed and some become clear; unobstructed beams must be selected and a smooth average must be produced.

(iii) The platform servo should, as far as possible, smooth out the angular fluctuations of the collimator beams due to atmospheric irregularities. It should also reduce as much as possible the effects of wind torques on the reference platform.

(iv) The platform servo in its turn is a vital element in the main telescope drive and control system, in that the platform provides the position of the telescope which is then (by comparison with the demanded telescope position) used to derive the error signals to control the main telescope drive. Thus, in simple terms, the platform servo and the main drive servo must work properly together.

(v) Small corrections must be applied to the autocollimator error signals if the tilt-sensors on the autocollimators indicate that ground movement has materially altered the collimator beam direction.

The servo-design proceeded in a straightforward manner. The reference platform has the following natural resonant frequencies:

| | | |
|---|---|---|
| Elevation axis | - | Torsional mode 200 Hz |
| | - | Bending mode 170 Hz |

| | | |
|---|---|---|
| Azimuth axis | - | Torsional mode 200 Hz |

and the following frictional torques:

| | | |
|---|---|---|
| Elevation axis | - | 0.08 foot pound |
| Azimuth axis | - | 0.06 foot pound |

From the frictional torques and the smallest acceptable angular hysteresis errors acceptable (0.5 arc second) the open-loop gain was derived. Tachometer compensation is used. The analysis shows that the torque motors are correctly chosen and that both servo loops (azimuth and elevation) will be stable and will have zero gain at a frequency of about 50 radians/second (8 Hz). This is satisfactorily below the lowest platform mechanical resonance frequencies and yet well above the zero-gain frequency of the main telescope drive servo.

(f) The overall reference platform system. Figure 23 shows in block diagram form the overall reference platform system. Most elements of it have already been described. The collimator selection is made using analog signals derived from the intensity of the collimator light beams; when a beam becomes obscured the signal from that collimator is removed from the averaging process. The collimator selector also, of course, receives the error signals from each collimator in digital form and passes these, after correction for tilt and after selection, to the error averaging block. The errors are generated simultaneously and separately in azimuth and elevation at a rate of 400 digital words per second.

The overall control of these elements of the platform system and the operation of the collimator selection and error averaging are functions of the main telescope control computer (this Chapter, Section 9).

## 8. The Drive and Control System

(a) General requirements. The means by which the telescope is driven and controlled must meet the following general requirements:

(i) The telescope must be capable of being smoothly driven in azimuth and elevation over the whole range of speeds necessary for accurate observations of radio sources in the sky. This implies a drive with good accuracy near zero velocity for both axes; the azimuth drive also needs adequate accuracy at high speeds so that the telescope can be used near the zenith.

(ii) The telescope motion must be controllable for a variety of observational programs either from commands supplied by the telescope computer or by manual control by an operator. The working coordinate system may be one of several sets of astronomical coordinates.

(iii) The telescope beam position, in astronomical coordinates, must be continuously measured and supplied, as a function of time, to

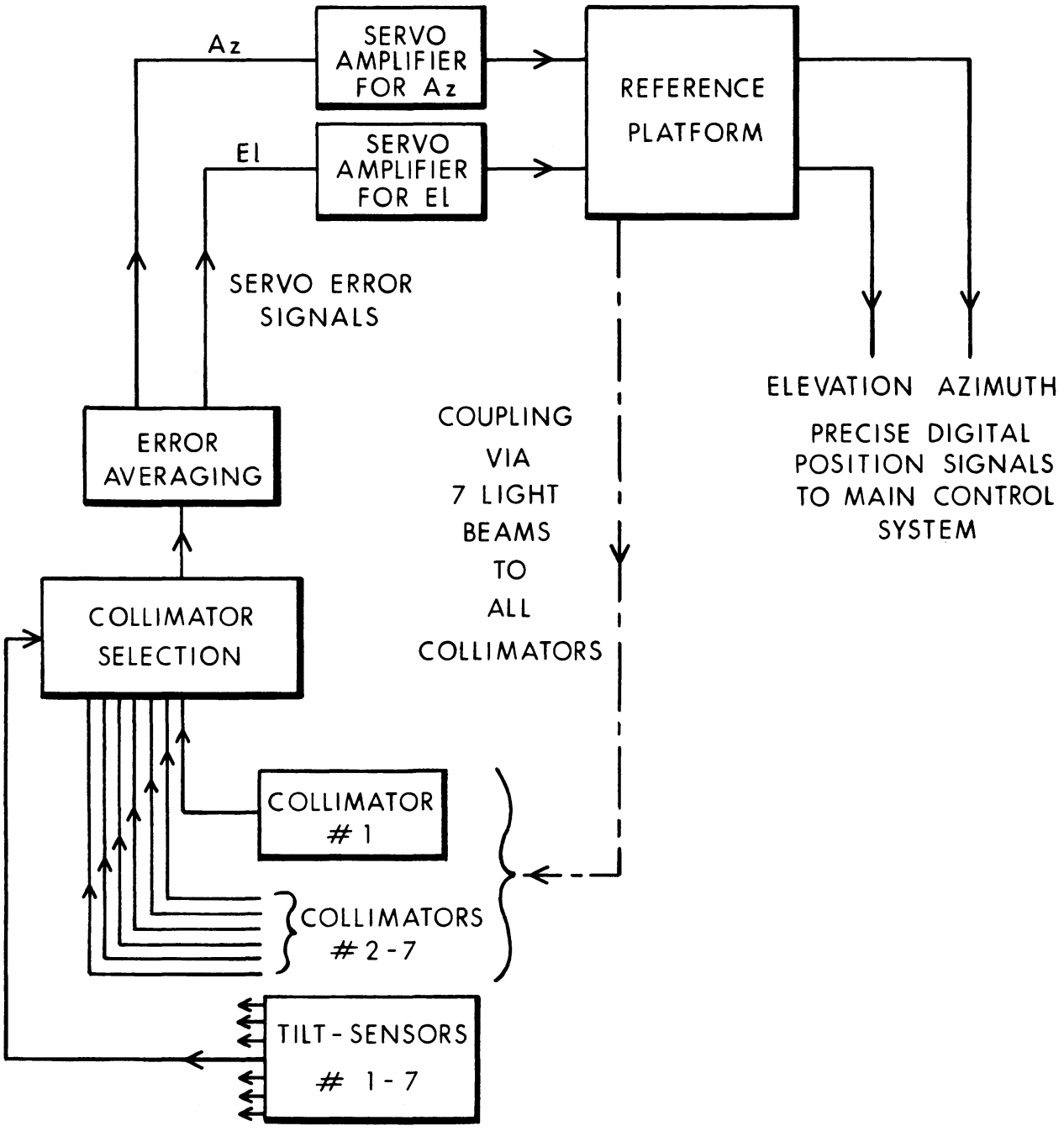


Figure 23. Block diagram of the reference platform control system.

the manual control console and to the telescope data recording system.

(iv) The telescope must move at slew speeds about both axes to go quickly from one position in the sky to another. This ability must be provided at all times and under all weather conditions up to these limiting conditions where the telescope must be driven to its stowed position. The slewing rates need not have any high positional or velocity accuracy.

The drive and control system has been designed to meet these requirements. More specifically it provides:

(i) A maximum drive rate of 20 degrees per minute at each axis.

(ii) The telescope can be driven to the stow position in winds up to 45 miles per hour.

(iii) The telescope will track any desired point in the sky (which is moving at or about the sidereal rate) with an angular accuracy ($1\sigma$ RMS) of 3 arc seconds, in winds up to 18 miles per hour. There is a cone of avoidance near the zenith where tracking is not possible; its semiangle is about one degree.

(b) The main drive components (SDL Report H-10, Chapters 7 and 11). Both the azimuth and elevation drive systems are electrical. The drive motors are air-cooled DC servo motors, driving through gear boxes. Both control servo loops employ velocity feedback and the main power drive is generated by solid-state amplifiers. There are 16 drive units for the azimuth drive and four for the elevation drive. The principle of using half the drive units to oppose the others ("bucking") to avoid backlash is used in both drive systems when they are used for precise driving. When used for slewing, all drive units supply torque in the required direction. Other methods of drive have been considered and none seem as good (either because of cost or performance) as the one selected.

The following two tables show the quantities which are used in selecting the main drive system and the components chosen.

Table 8. Azimuth Drive Parameters

| Property | Value |
|---|---|
| Moment of inertia at azimuth axis | $6.1 \times 10^9$ in.lb. sec$^2$ |
| Maximum wind moment (18 miles per hour wind) for precise tracking | $1.0 \times 10^6$ ft. lbs. |
| Maximum acceleration moment during tracking | $0.89 \times 10^6$ ft. lbs. |
| Maximum friction moment during tracking | $0.177 \times 10^6$ ft. lbs. |

Table 8, continued

| Property | Value |
|---|---|
| Maximum rolling friction moment | $0.083 \times 10^6$ ft. lbs. |
| Drive-to-stow moment (45 miles per hour wind plus friction) | $7.0 \times 10^6$ ft. lbs. |
| Maximum slew speed | 19.7 degrees per minute |
| Number of drives | 16 |
| Mean radius of azimuth turntable | 123.00 feet |
| Diameter of drive wheel | 36.0 inches |
| Gear ratio of drive train | 189.5:1 |
| Overall drive ratio (input-shaft to azimuth axis) | 15,538:1 |
| Maximum speed of input shaft | 850 RPM |
| Static efficiency of gear train | 95% |
| Dynamic efficiency of gear train | 98% |
| Spring constant of a single gear train at the input shaft | $3.6 \times 10^3$ in. lbs./radian |
| Moment of inertia of gear train at the the input shaft | 0.125 in. lb. $sec^2$ |
| Horsepower of a drive motor, its frame and type | 5 HP at 850 RPM. Frame 286D, 240 V-DC fan cooled, totally enclosed GE compensated DC servo motor. |
| Type of drive system | Anti-backlash (8 driving, 8 bucking except when slewing) |

Table 9. Elevation Drive Parameters

| Property | Value |
|---|---|
| Moment of inertia at elevation axis | $1.6 \times 10^9$ in. lb. $sec^2$ |
| Maximum wind moment (18 miles per hour wind) for precise tracking | $1.0 \times 10^9$ ft. lbs |
| Maximum acceleration moment during tracking | $0.23 \times 10^6$ ft. lbs. |
| Maximum friction moment during tracking | $0.066 \times 10^6$ ft. lbs. |
| Drive-to-stow moment (45 miles per hour wind plus friction) | $6.5 \times 10^6$ ft. lbs. |
| Maximum slew speed | 22.4 degrees per minute |
| Number of drives | 4 |
| Pitch radius of ring gear | 794 |
| Pitch diameter of drive pinion | 13.60 inches |
| Gear ratio of drive train | 117.18:1 |
| Overall drive ratio (input shaft to elevation axis) | 13,683:1 |
| Maximum speed of input shaft | 850 RPM |
| Static efficiency of gear train | 95% |
| Dynamic efficiency of gear train | 98% |
| Spring constant of a single gear train at the input shaft | $2.32 \times 10^4$ in. lbs./radian |
| Moment of inertia of gear train at the input shaft | 1.9 in lb. $sec^2$ |
| Horsepower of a drive motor, its frame and type | 20 HP at 850 RPM. Frame 368 D, 240 V-DC fan-cooled, totally encloded GE compensated DC servo motor |
| Type of drive system | Anti-backlash (2 driving, 2 bucking, except when slewing) |

Both drive systems require gear reducers, and these must meet requirements both for transmitting the maximum torque required to move the telescope in winds and also for adequate stiffness to give a high spring constant to the total structural resonance. The azimuth gear trains have been specially designed (Drawing 111-D-008, Sheet 3). For the elevation drive it has been possible to select gear boxes (Western Gear No. 44125-RI) which have been designed for antenna applications and have high efficiency, low inertia, good stiffness and small size. Brakes are mounted on each gear box.

The tachometers needed for the velocity feedback loop of the servo are mounted on all the 16 azimuth and 4 elevation drive units.

The remainder of the azimuth drive components have already been described, so that only a brief further description is needed of the elevation drive and the bull gear.

To preserve the homologous behavior of the reflector structure, it is important that no large loads (greater than about $\pm$ 5000 pounds) be applied radially to the elevation wheel by the elevation drive. Also, to keep the lowest natural resonant frequency of the reflector structure high, it is most desirable that the mass of the elevation drive assembly not contribute to the reflector structure moment of inertia. These two requirements have been met by (1) floating the elevation drive on the elevation gear, (2) balancing the weight of the drive assembly by spring-tension devices, (3) arranging that the spring-tension cylinders are critically damped. The elevation drive arrangement is shown in drawings Nos. 111-D-005, Sheets 1-4, and a further detailed description is in SDL Report H-10, Chapter 8.

The main elevation gear has a pitch radius of 66 feet 2 inches, a 1.25 inch pitch and a face width of 8 inches. The gear support girder is shown on drawing No. 111-D-001, Sheet 3.

(c) The design of the control system. The telescope drives are fed with power from the servo system in such a way that whenever there is an error between the actual telescope position and its required position the servo supplies drive torques to correct this error. The general requirements for such a servo system are that it should give a stable and accurate drive. The conditions that are taken into account in making such a design may be outlined as follows:

(i) The dynamical properties of the structure to be driven must be known. Any well-built elastic structure will be capable of oscillations in a variety of modes, and usually these modes show very little damping. Thus the modes must be discovered and their natural frequencies determined so that the drive can be designed to avoid exciting any of the possible oscillations. (The dynamic analysis of the present structure is treated in more detail in Chapter III, Section 2.)

(ii) The main mechanical disturbances which can influence the accuracy of the drive system are frictional torques and the varying

torques on the structure due to wind. The servo must thus deliver sufficient drive torque to overcome frictional torques when the positional error of the telescope is small compared with the required tracking accuracy. Also, the servo must be capable of responding to positional errors induced by wind; this requires that the range of frequencies over which it performs well should cover most of the frequency range within which the wind can induce pointing errors.

Of course, analysis and experience is used in the overall telescope design to ensure that the servo can meet its requirements. For example, the structural and mechanical design of the present telescope was initially required to yield no oscillatory modes with natural frequencies below 1.5 Hz. This figure is related to the frequency range of the wind-induced torques which begin to fall off in magnitude at about 0.02 Hz and fall quite rapidly above 0.3 Hz. It is a good working rule that the servo frequency bandwidth can extend from zero frequency up to one-third or one-fourth of the lowest structural frequency. Similarly, the frictional forces (both static and rolling) of the azimuth and elevation movement were estimated early, so that the servo design would be able to handle the resulting frictional torques.

(d) Design method and results. With these considerations in mind, let us look in rather more detail at the steps which the servo design has followed. (See Figure 24 for a block diagram of a simple servo loop.)

The steps followed in the design are:

(i) The magnitude of the error signal, in millivolts, which corresponds to a one-bit (0.31 arc seconds) telescope position error, is determined and arranged to be adequate when compared to the electronic noise at the preamplifier input.

(ii) The gain of the amplifier chain must be sufficient so that this error signal can produce a torque at the drive motor shaft sufficient to overcome friction and operating wind torques at that point. Since these torques and the motor characteristics are known, the amplifier gains are determined. A check is then made to ensure that sufficient motor voltage can be supplied to drive at full motor speed.

(iii) Using the transfer function of the servo motor and tachometer feed-back, the transfer function of the compensation network required to give a stable servo system is derived.

At this stage, for example, the azimuth axis drive design had an open-loop gain of 47 dB and a phase margin of 35° at the frequency of 4.5 radians per second (0.7 Hz) where the open-loop gain becomes equal to unity. These values satisfy the requirements of stability and of satisfactory performance in the presence of friction. This latter point was, however, analyzed in more detail, and so also was the performance of such a servo loop in the presence of wind disturbances.

The analysis of the effects of friction was quite detailed (SDL Report H-10, Chapter 11, Sections 9 and 10). Two effects were discussed:

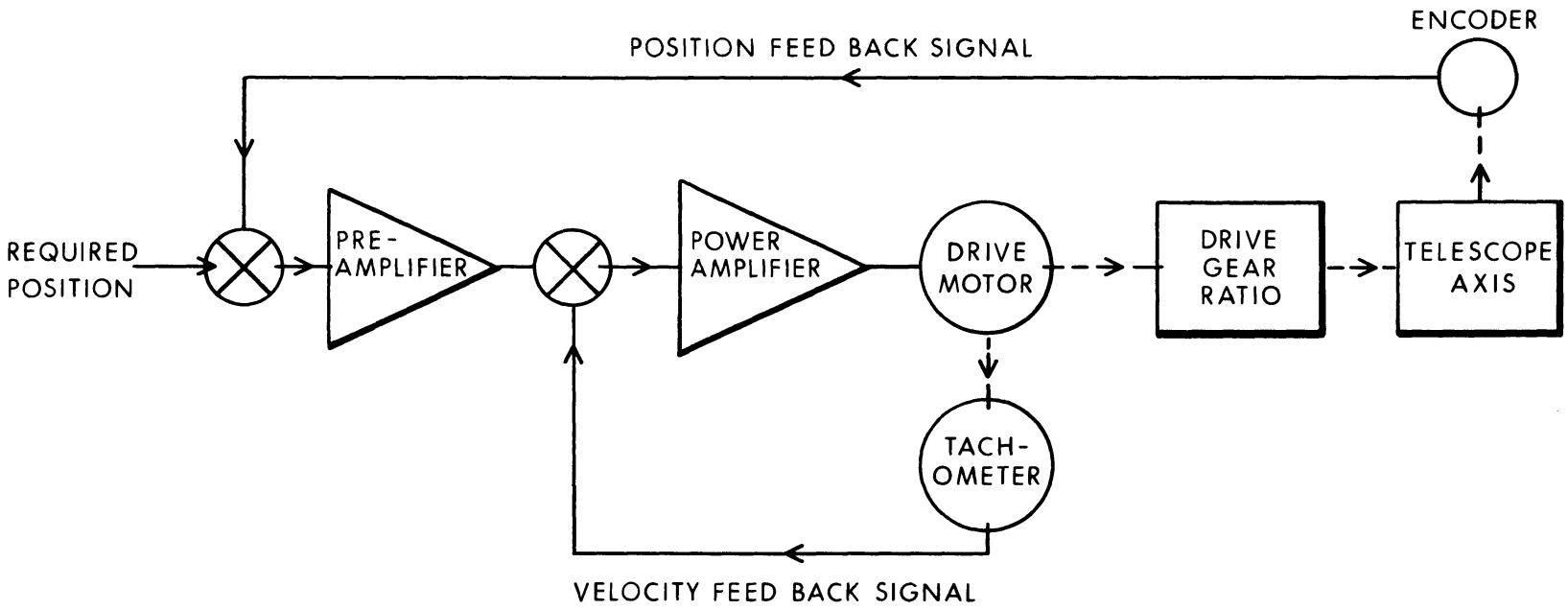


Figure 24. A block diagram of the servo drive for one axis of the telescope.

"stick-slip" and "limit cycling". Stick-slip is the phenomena which occurs because static friction is normally greater than rolling friction; there is thus the possibility that the drive will go in a succession of jumps in position at low speeds. A servo with velocity feedback may show limit cycling, which means that the telescope position may oscillate about the required position as the instrument moves. This effect also depends on the sliding-rolling friction difference.

The results of the analysis showed that both effects will occur, but that they result in pointing errors of about 0.5 arc seconds occurring at frequencies about 0.3 Hz. (More precise figures are included in the pointing error budget in Chapter III.) Errors of this magnitude are quite acceptable.

The final stage in the design was the choice of the various main components, e.g., amplifiers, motors and tachometers, to be used in the servo-system. No difficulties were experienced in this task since the realization of the system falls within the state of present-day practice.

(e) The operational control. Figure 25 shows in a simplified form one element of the drive and control system, as, for example, would be employed to drive two of the four elevation drive pinions. The main commands come from the computer (which is described in the following paragraph), but they may also be commands by an operator at the control console. The command is compared, in the digital subtractor, with either the error-corrected precise telescope position derived from the reference platform or with the coarse position from the axis encoder. The error signal goes via a torque equalizer (whose task is to ensure that all drive units contribute approximately equally to the drive load) to the drive-buck difference control. This control sets the right difference between the torque developed by the motor which is driving in the required direction and the motor which is cancelling backlash by opposing the drive. (In slew, this control drives both motors together.) Each motor and its associated tachometer has its own servo amplifier and drives its own gear reducer. The output shafts of the two reducers drive (and buck) the drive to the telescope axis.

This system is typical of both the azimuth and elevation drives. In azimuth, there are eight such pairs of drive motors driving 16 wheels; in elevation two such pairs drive four pinions on the elevation bull gear.

## 9. The Telescope Computer

There are many tasks for the telescope computer; in this section we will outline these and give some indication of their complexity. The telescope computer will not, however, handle the observational data from the telescope, as that will be the task of the data-handling and process-

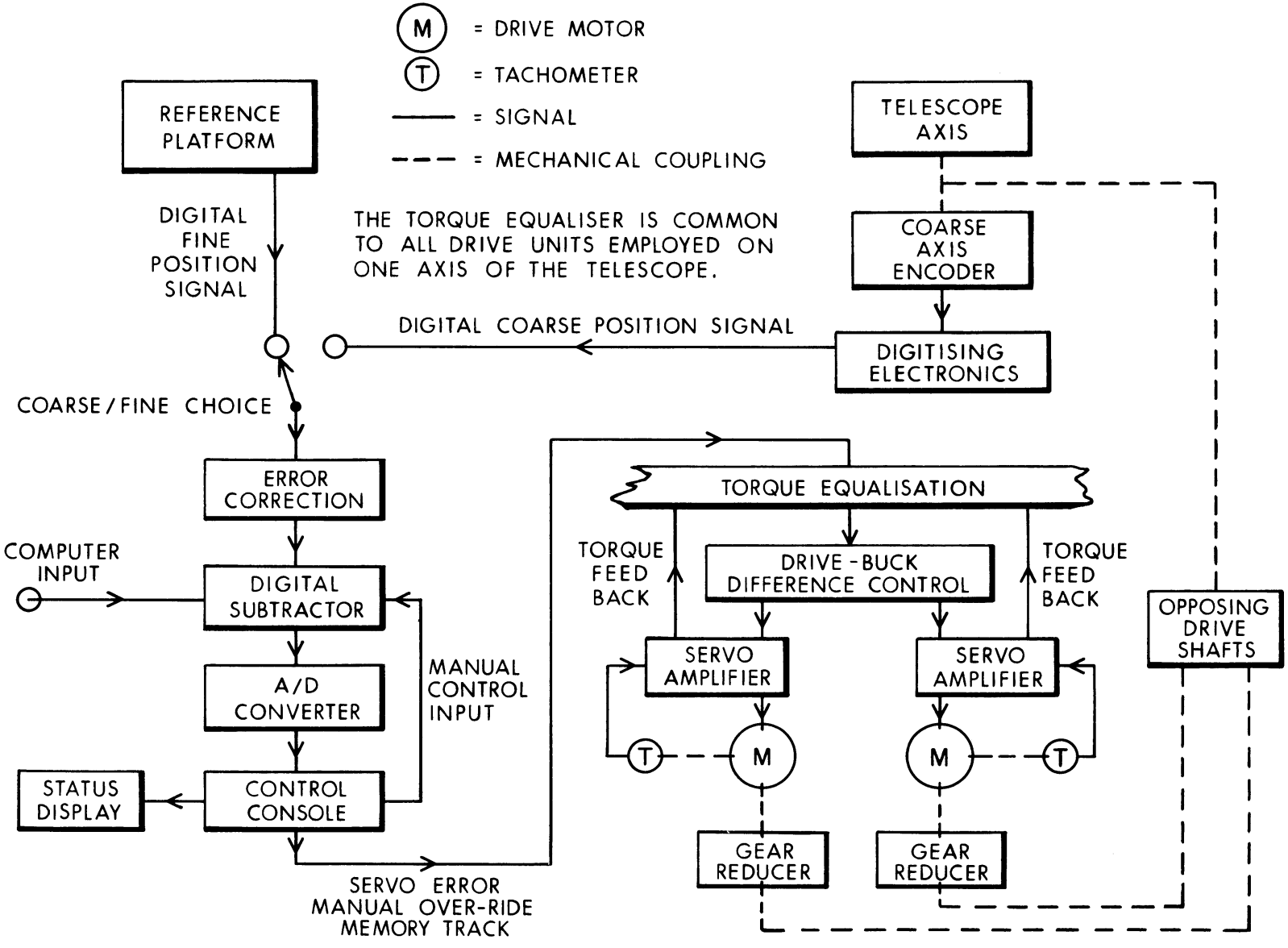


Figure 25. Block diagram for one unit of the drive and control system.

ing computer. The two computers will communicate with each other, but this separation of functions is very desirable and, owing to the development of several good, small-sized computers, not expensive. It means that the telescope computer can be programmed, tested and set into operation and then not be subject to changing requirements. The data-processing computer will require quite considerable flexibility to cope with changes in observing methods and different scientific tasks. This separation of function also allows us to reserve the choice of the data-handling computer to a late stage. It is therefore not considered further here; its cost will be included in the cost of the electronic observing equipment for the telescope.

The following are the chief computer tasks:

(a) Reference platform orientation. The computer will continuously calculate the orientation of the stable reference platform. This orientation provides the basic coordinate system for the telescope; source positions or required beam positions of the telescope are transformed into this coordinate system and compared with the telescope position to generate the error signals for the drive. The orientation of the platform is also required as an input to the platform servo to maintain the platform angular stability. This computer task may be further described as the following subtasks:

(i) Setting up and inverting the matrices relating the active autocollimator outputs (there will be between 4 and 14 outputs active at any one time) and deriving the least squares solution for the platform altitude and azimuth.

(ii) Performing the matrix multiplication needed to solve for the platform orientation given the autocollimator outputs.

(b) The telescope position. The computer will calculate continuously the desired telescope position in the reference platform coordinate system. Such a calculation is a spherical transform, and can be made without excessive effort for a variety of coordinate systems. The desired telescope position will be the input; it will be possible to insert it in any of the following coordinate systems:

(i) Altitude and azimuth.
(ii) Hour angle and declination.
(iii) Right ascension and declination.
(iv) At any epoch after 1850 in equator and equinox coordinates.
(v) Ecliptic coordinates.
(vi) Galactic coordinates (old and new).

The results of this calculation goes via a buffer to the digital comparator where it is compared with the stable platform encoder outputs.

(c) Pointing corrections. The computer will apply pointing corrections which are known to exist, from prior calibrations of the telescope, and those due to atmospheric refractivity. For this latter calculation the computer is supplied with measurements of ground-level

temperature, barometric pressure and relative humidity. The pointing corrections due to the structure are slowly-varying functions of the elevation angle and are easily dealt with. The computer will provide an output to adjust the subreflector or prime focus feed position as a function of elevation angle so that the changing focal length of the telescope as it tilts can be allowed for.

The rapidly varying (but small) reproducible errors inherent in the precision encoder system are compensated in the electronics associated with the encoders and not in the computer.

(d) Other tasks. The following various tasks will be handled by the computer:

(i) It may be desirable to display telescope coordinates in a system different from the one chosen as computer input. The computer must make the transform and send the coordinates to the display in the correct form (angles must be in degrees, minutes and seconds, for example).

(ii) The computer will calculate the parallactic angle for the telescope beam in the sky. This is needed for polarization observations, and may in fact be used either to control the orientation of the telescope feed or to provide as output data the relation between feed orientation and the source orientation in the sky.

(iii) Already, in (b) above, the computer has control of the telescope position and can command it to follow a variety of tracking or scanning demands. However, it must also be possible for the operator to insert manually a position change in case he wishes to make a manually controlled scan in any coordinate system. The computer meets this task, which is not met by the existing ability to transfer full control from the computer to the telescope operator.

(e) Other control system modes. The computer would be capable of carrying out the following two functions, although the present design of the control system does not require it to do so:

(i) The computer could calculate the velocity required for any change in the telescope position and supply this as a velocity signal to the servo loop. This mode can be an improvement over the more straightforward provision of velocity information derived from the tachometers.

(ii) The comparison of actual-demanded telescope position could be made digitally in the computer rather than in the digital comparator and the positional error processed digitally. This could make it simpler to achieve the desired network response in the servo-loop.

Each of the above computer tasks has been used to give an estimate for its running time and frequency of operation. These estimates have been based on a 2 microsecond core cycle and an instruction set typical of small 16-bit computers. The required input-output devices have also been listed.

There will also be programs for acquisition of reference platform lock (for use after the shut-down, for example), a variety of programs to test and exercise the main and platform servos and other similar tasks.

The general intent is that, after test and debugging, all programs would be coded into read-only memory and the computer inhibited from executing instructions from the remaining core scratch pad. The computer would thus be protected from destroying its own program memory, and its operating instructions would consist only of turning it on.

## References


Findlay, J. W. 1971, Ann. Rev. of Astron. and Astrophys., 9, 271-292.

Froome, K. D., and Bradsell, R. H. 1966, J. of Sci. Instruments, 43, 129-133.

Kühne, C. 1966, in "Design and Construction of Large Steerable Aerials", Institution of Electrical Engineers (GB) Conference Publication No. 21, pp. 187-198.

Kurtz, R. L., and Hayes, J. L. 1966, "Experimental Measurement of Optical Angular Deviation Caused by Atmospheric Turbulence and Refraction", NASA Technical Note TN D-3439, National Aeronautics and Space Administration, Washington, D. C.

Leitz, H. 1969, "Two Electronic Tacheometers by Zeiss", translated into English from Allgemeine Vermessungs-Nachrichten, 76, pp. 73-79.

Saastamoinen, J. J. 1967, Surveyors Guide to Electromagnetic Distance Measuring, University of Toronto Press, Toronto, Canada.

von Hoerner, S. 1967(a), Astron. J., 72, 35-47.

von Hoerner, S. 1967(b), J. Struct. Div. Proc. Amer. Soc. Civil Engrs., 93, 461-485.

von Hoerner, S. 1969, in "Structures Technology for Large Radio and Radar Telescope Systems", James W. Mar and Harold Liebowitz, eds., MIT Press, Cambridge, Mass., pp. 311-333.